X-693-73-346
PREPRINT

NASA TM X- 70540

SATELLITE OBSERVATIONS OF TYPE III SOLAR RADIO BURSTS AT LOW FREQUENCIES

JOSEPH FAINBERG
ROBERT G. STONE

NOVEMBER 1973

GODDARD SPACE FLIGHT CENTER
GREENBELT, MARYLAND

TO BE PUBLISHED IN SPACE SCIENCE REVIEWS

SATELLITE OBSERVATIONS OF TYPE III SOLAR RADIO BURSTS AT LOW FREQUENCIES

by

Joseph Fainberg and Robert G. Stone
Radio Astronomy Branch
Laboratory for Extraterrestrial Physics
Goddard Space Flight Center
Greenbelt, Maryland

ABSTRACT

Type III solar radio bursts have been observed from 10 MHz to 10 kHz by satellite experiments above the terrestrial plasmasphere. Solar radio emission in this frequency range results from excitation of the interplanetary plasma by energetic particles propagating outward along open field lines over distances from 5 $R_\odot$ to at least 1 AU from the sun. This review summarizes the morphology, characteristics and analysis of individual as well as storms of bursts. Substantial evidence is available to show that the radio emission is observed at the second harmonic instead of the fundamental of the plasma frequency. This brings the density scale derived by radio observations into better agreement with direct solar wind density measurements at 1 AU and relaxes the requirement for type III propagation along large density-enhanced regions. This density scale with the measured direction of arrival of the radio burst allows the trajectory of the exciter path to be determined from 10 $R_\odot$ to 1 AU. Thus, for example, the dynamics and gross structure of the interplanetary magnetic field can be investigated by this method. Burst rise times are interpreted in terms of exciter length and dispersion while decay times refer to the radiation damping process. The combination of radio observations at the lower frequencies and in-situ measurements on non-relativisitic electrons at 1 AU provide data on the energy range and efficiency of the wave-particle interactions responsible for the radio emission.

INTRODUCTION

Low frequency solar radio bursts originate from particle-field-plasma interactions occurring in regions from 5 solar radii ($R_\odot$) to 1 AU and beyond. These are regions where the coronal properties change from the rigid rotation conditions near the solar surface to the corotating conditions in the interplanetary medium. With increasing distance from the sun the solar plasma density, temperature, and collision rate decrease, the bulk speed increases, and the corona takes on the flow characteristics of the solar wind. The magnetic fields change from predominantly closed configurationsnear the solar surface to predominantly open configurations farther out.

Travelling type III radio bursts which are generated by energetic particles moving outward along open field lines from their acceleration region provide a very important and unique source of information about physical conditions along the path of the exciter particles. In many cases these radio measurements provide a link between the observations of phenomena occurring near the solar surface and the extensive in-situ observations of solar wind,

particles, and magnetic fields near 1 AU. However, it is important to note that the observed type III bursts can originate in regions well out of the ecliptic plane, thus furnishing data about extensive remote areas not accessible to direct space probes.

Ground based radio observations are limited essentially to frequencies above 10 MHz. For lower frequencies it is necessary to use space platforms above the obscuring ionosphere and for the lowest frequencies it is necessary to make measurements at locations within the solar wind. The number of such space experiments has been small but the value of the data for remote exploration of the interplanetary process is becoming increasingly evident as new observational and data processing techniques evolve. Such techniques now permit the radio tracking of energetic particles in flight as they move outward from the sun (Fainberg et al., 1972) and provide for the first time a means of visualizing and measuring the gross magnetic field configuration through large volumes of interplanetary space.

This review will concentrate on spacecraft observations of solar phenomena made at frequencies below 10 MHz. In

certain cases the data will be compared to observations at higher frequencies to illustrate the connection and evolution of common phenomena. For general reviews covering higher frequency observations in detail see Wild et al. (1963), Kundu (1965), Wild and Smerd (1972), Rosenberg et al. (1973).

In part 1 a discussion is given of the general problems associated with spacecraft observations along with a brief history of such experiments. In part 2 the morphology of type III bursts and storms is discussed with summaries of observed characteristics. Part 3 contains a series of analyses which have been made utilizing hectometric and kilometric data to obtain properties of the burst emission process and the interplanetary medium.

1. EXPERIMENT CONSIDERATIONS

1.1 Design Constraints

The most common form of solar radio burst is the type III burst characterized by a rapid drift in time from high to low frequencies. Type III bursts have been interpreted (Wild et al., 1963) as resulting from the interactions of a group of charged particles (exciters) moving along magnetic field lines through the coronal plasma

into regions of decreasing density. The fast particles excite plasma oscillations of the medium at progressively lower frequencies. The plasma waves are partially converted to electromagnetic waves which may be detected at large distances from the source region. The intensity-time profile of the radio burst at a particular frequency contains, therefore, information on the physics of the exciter-plasma interaction at a particular level in the corona.

For example, the rise time of the burst is related to the length of the exciter. The burst intensity reflects the number of particles in the exciter as well as the efficiency of the conversion and propagation processes. The burst decay represents the damping of the plasma oscillations and may yield information on the coronal electron-proton interactions. The path of the radio burst emission regions outlines the gross magnetic field because of the small gyroradius of the exciters even near 1 AU.

The experimental task is to obtain the intensity-time profiles over a wide range of frequencies (dynamic spectra) which then provide a measurement of these various physical processes as the exciter moves outward. If, in addition,

the burst origin can be located,then the coronal densities and interplanetary magnetic field configurations can be determined along the burst path. Because of the large number of bursts observable, with rates of thousands per day at active times, the slowly-varying as well as average properties of the interplanetary medium can be studied in this manner by radio techniques.

At frequencies above 10 MHz many measurements of the complex phenomena near the sun have been made at the increasingly large groundbased antenna installations. At decameter wavelengths, for example, multielement interferometers with baselines of several kilometers have been used (Kundu, 1965).

Spacecraft experiments, however, have severe limitations on weight, size, power, and telemetry data rate. Each of these factors serves to restrict the variety, quality and volume of data brought back to ground observers for analysis. Spacecraft subsystem radio frequency interference (RFI) most often occursin the low frequency band and can saturate the radiometers or greatly decrease their sensitivity and dynamic range. The suppression of RFI requires careful

design and testing of all spacecraft electronic subsystems.

Size, weight and technological considerations greatly restrict the receiving antenna systems to dipoles which are short compared to wavelength and which possess poor angular resolution. The available telemetry data rate greatly restricts the number of observing frequencies and the sample rate. Fortunately the radio bursts lengthen in time at low frequencies so that the sampling rate necessary to measure burst properties is reduced. However a wide dynamic range of the receivers, along with adequate amplitude resolution place great demands on the available telemetry data rate and this usually forms the most pressing constraint in modern experiments.

1.2 History of Satellite Observations

Ground based observations of solar radio bursts have been extended by Sheridan and Attwood (1962) down to 5 MHz, although generally the cutoff imposed by the terrestrial ionosphere is about 10 MHz. A radio astronomy experiment proposed by the University of Michigan as early as 1960 was flown on the OGO-1 satellite launched in 1964. Due to an unfortunate combination of spacecraft system failures,

however, no solar bursts were observed with this experiment. The first spaceborne observations of solar radio bursts at low frequencies were obtained by Hartz (1964) in the frequency range 1.5 to 10 MHz using a receiver on the Alouette-1 satellite. Hartz found that type III events which appeared to originate at altitudes out to about 10 $R_\odot$ were observable with the short dipole antenna and frequently had intensities in excess of 10 db above the cosmic radio noise background. Slysh (1967a,b) obtained observations of solar bursts at 0.2, 1, and 2 MHz using the Zond-3 and Venera-2 data, and Stone et al. (1968) obtained observations at 0.45 and 3 MHz with the ATS-2 satellite. A swept frequency receiver covering the range 4-2 MHz was flown on OGO-3 in 1966. Between June 7, 1966 and September 1967, 218 solar bursts were detected by this experiment (Haddock and Graedel, 1970). Additional observations were obtained from the Alouette II satellite in the 1 to 10 MHz region and reported by Hakura et al. (1969). More detailed studies of the early satellite observations of low frequency solar bursts have been published by Hartz (1969), Alexander et al. (1969), and Haddock and Graedel (1970).

Because these observations were made with dipole antennas, the source locations of the radio emission were not known and the results were very model dependent. For example, assuming that an exciter speed of the order of c/3 observed at higher frequencies persisted at larger distances from the sun and that the observed radio emission occurred at the fundamental of the local plasma frequency, then from these early observations of dynamic spectra it was concluded that the observed type III bursts were generated in regions of density enhancements (streamers) associated with active regions which extended out to at least 50 $R_\odot$ in the corona (Hartz, 1969; Alexander et al., 1969). Furthermore, if the burst decay were due solely to collisional damping the same analyses suggest that within the density enhancements the electron temperature appeared to fall off more rapidly with distance than in the ambient solar wind. As these conclusions were extended out farther with still lower frequency observations, it became clear that a serious discrepancy existed between the results obtained by radio observations and those obtained by other techniques including direct measurements at 1 AU.

The radio astronomy explorer (RAE-1) launched in July 1968 was the first satellite devoted entirely to radio observations at low frequencies. The spacecraft provided an essentially RFI-clean environment for the observations of cosmic radio noise as well as solar bursts in the frequency range from 0.2 to 9 MHz. The satellite, described elsewhere, (Weber et al.,1971) carried two 228-meter-long V antennas for the study of the cosmic and terrestrial noise background, as well as a dipole antenna for integrated cosmic noise and solar burst observations. By the time that the spacecraft experiments were turned off in 1972, many hundreds of thousands of type III bursts had been observed to occur as individual and complex events and as storms of thousands of bursts lasting for many days (Fainberg and Stone,1970a).

The successful operation of the University of Michigan multifrequency radiometer on OGO-5 extended the range of observations of solar bursts to 50 kHz (Haddock and Alvarez, 1973). Type III bursts observed on OGO-3 down to 25 kHz were reported by Dunckel et al. (1972). The lowest frequency to date at which a Type III burst has been detected is 10 kHz by the University of Minnesota plasma wave experiment on IMP-6 (Kellogg et al., 1973).

An ingenious technique for determining radio burst source directions was described by Slysh (1967c). He utilized the direction finding capability afforded by spin modulation as well as lunar occultation to obtain type III source directions from data from the Luna 11 and Luna 12 probes at 1.0 and 0.2 MHz. Slysh concluded that at these frequencies the source locations for several large solar events were 30-40 $R_\odot$ and 200 $R_\odot$, respectively, from the sun. The results were somewhat limited by low sensitivity of the short antenna and knowledge of the beam pattern (2.5-m rod plus housing inclined to the spacecraft body) and by limited information on spacecraft orientation.

The IMP-6 satellite (launched March, 1971) provided the first opportunity to do extensive direction finding of radio sources utilizing spin modulation. On this spacecraft a high sensitivity was provided by long dipole antennas (92 m). Accurate aspect information ($< 1^o$) was obtained from optical sensors, and extensive frequency coverage from 10 MHz to well below 10 kHz was provided by instruments of several experimenters (Goddard Space Flight Center, University

of Minnesota, University of Michigan, and University of Iowa). In addition, this spacecraft included a fast electron analyzer (University of California) and proton analyzers (Goddard Space Flight Center and Applied Physics Laboratory of Johns Hopkins University) yielding simultaneous measurements of energetic solar particles. Some of these burst-associated particle results are described later in part 3.

In July, 1973, RAE-2 was launched into lunar orbit. The GSFC experiment aboard this satellite will provide additional information on source locations and sizes derived from lunar occultations over a wide range of frequencies down to 25 kHz.

Future radio astronomy experiments are planned for HELIOS A (1974 mission going in toward the sun to 0.3 AU), IME (1978 mission with a radio experiment determining out-of-ecliptic source directions), and MJS (1978 deep space probe to beyond 5 AU).

2. OBSERVABLE BURST CHARACTERISTICS

2.1 Morphology of Bursts

This section describes the observable characteristics of solar bursts which have been used in summarizing a large volume of data in terms of parameters useful for further analysis. For this it is necessary to discuss some general

aspects of the burst morphology and to indicate what parameters have been most relevant. It is important to realize that each experimenter selects sample phenomena to study and interpret. It is not always evident how typical such samples are of the larger volume of raw data.

The most obvious characteristic of type III bursts is the rapid time drift from high to low frequencies. The bursts have been measured over frequencies extending from hundreds of MHz down to frequencies near 10 kHz (Kellogg, 1973) corresponding to emission levels located at distances from several tenths of a solar radius above the photosphere to beyond the earth's orbit. At each frequency, simple bursts are characterized by a rapid rise followed by a somewhat slower decay. There are usually cutoffs associated with both ends of the frequency range for individual bursts. Some bursts are not observable at frequencies above a certain value which may be below 1 MHz. Other bursts may be observable only down to a frequency which may be above 100 MHz. A small sample of large bursts is observable over the full range of frequencies. It is likely that the cutoffs contain significant information on local emission and propagation conditions.

Figure 1a (Fainberg and Stone, 1970a) shows an example of a type III burst drifting from 5.4 MHz to below 0.5 MHz. The upper figure is a plot of the dynamic spectrum in 1 db intensity contours above background. The lower figure is a plot of intensity-time profiles for 6 separate frequencies from a different receiver. The features of this burst which characterize many bursts are evident: frequency drift, abrupt onset followed by a slower decay, and a high frequency cut-off. Figure 1b shows a more common situation where several bursts occur closer together. Note that the different members of the group have different dynamic spectra; the high frequency cutoff of the first burst is distinctly lower than that of the second burst of the group. Since type III bursts usually occur in groups this illustrates the difficulty in measuring parameters like drift rate and onset times over a wide frequency range without very good frequency, intensity and time resolution. For this example it would be difficult to determine relevant burst parameters if the measured frequencies were separated by octaves. The low frequency cutoff in both figures is due to refraction in the ionosphere above the RAE-1 satellite.

In addition to isolated bursts and groups of bursts, there are also the phenomena of hectometer solar storms (Fainberg and Stone, 1970a,b, 1971a) consisting of hundreds of thousands of drifting bursts associated with a particular active region on the sun. Figure 2 shows the dynamic spectrum of solar radio emission near the time of central meridian passage (CMP) of the associated active region. The burst occurrence rate at 2.8 MHz is about 1 burst every 10 sec. The dynamic spectrum for this storm recorded four days earlier is given in figure 3. The lower observed activity is more likely due to refractive beaming by the corona which tends to focus the EM radiation in the direction of steepest density gradient, rather than to changes in source activity; similar CMP effects are observed with other active regions. These figures also indicate the increase in burst frequency drift rate near CMP, the analysis of which is described in part 3.

In addition to the large number of type IIIs, a continuum component of hectometric storms has also been reported (Fainberg and Stone, 1971b). Figure 4 (Stone and Fainberg, 1973) shows plots of average flux and minimum flux for successive 10-minute intervals during the August 1968 storm. The minimum flux plots represent background levels between

individual type III bursts and show that in addition to the thousands of discrete exciters there is also a quasi-steady particle component capable of generating radio waves. Evidence from the IMP-6 spacecraft described in part 3 indicates that the source emission levels of the storm continuum component are similar to the source emission levels of the type III's.

2.2 Burst Parameters

In order to summarize the large number of bursts for further analysis it is necessary to define and measure the distribution of quantities which characterize the bursts. There is usually an implicit assumption that groups of bursts and storms of bursts are made up of overlapping bursts, and that the study of the simple non-overlapping bursts adequately describes the complex situations. Isolated bursts generally make up only a few percent of the total and there is the possibility that other phenomena are involved at periods of high activity*. In any event most data now available pertain to analyses based on simple type III bursts.

*Type II bursts associated with interplanetary shocks have been reported (Malitson et al., 1973a).

Figure 5 (Evans et al.,1973) shows an intensity time profile of a representative burst in detail. Such bursts can be characterized by a rapid rise from background levels to a single peak followed by a slower exponential decay. Parameters useful for describing the bursts are listed below:

(1) Onset time - the time at which the burst rises above background. For quiet background conditions this time is fairly well defined. However,when the background varies considerably because of magnetospheric noise or because of small solar bursts often present,this time may not be accurately determined. The onset time generally reflects the arrival at the appropriate coronal level of the more energetic particles comprising the exciter. It also includes the radio propagation time to the observer.

(2) Peak time - the time of the burst maximum. This is usually well defined except when the receiver saturates. It depends on the arrival of the more numerous slower exciter particles at the appropriate

emission level and also includes the radio propagation time to the observer.

(3) Burst excitation time (t_e) -time measured from the burst onset time to the time past the peak when the observed exponential decay just becomes linear on a log plot. Aubier and Boischot (1972) show that this time can be interpreted as the duration of the exciter at a particular coronal level.

(4) Burst decay time (t_d) - time taken for the emission to decay by a factor of e^{-1} during the exponential decay. It is important to note that most simple bursts show a nearly exponential decay extending for large bursts over 4 or 5 decades of intensity. Most observers believe that negligible excitation is present during this decay phase.

(5) Burst intensity - peak intensity of the burst measured in flux at the antenna or in terms of an equivalent antenna temperature. This quantity depends on the exciter-plasma-electromagnetic radiation conversion processes as well as on the propagation conditions to the observer.

(6) Burst onset drift rate - frequency drift rate of the onset times of a given burst. This quantity is available only when there are clear onset times. Because of the radio propagation time, the burst onset drift rate depends on the exciter direction relative to the observer.

(7) Burst peak drift rate - frequency drift rate of peak times of a given burst. This quantity is usually well defined. It also depends on the orientation of the exciter direction to the observer.

(8) Burst occurrence rate - number of bursts observed per unit time. This can be determined when the bursts do not overlap severely. Solar storms appear to have a different burst distribution of amplitudes (more small ones) than bursts associated with flares. The burst occurrence rate depends on the existence of active regions and is likely to vary extensively with activity in the solar cycle.

(9) Burst arrival direction - average direction of arrival of the solar burst with respect to the observer-sun line. Recent data processing techniques permit this quantity to be determined

from spin modulated spacecraft data (even with short dipoles) to within one-degree accuracy (Fainberg et al., 1972). The determination of this information has allowed radio bursts to be tracked out to 1 AU from the sun.

(10) Background level - level before and after burst. Bursts are observable only when they are above the background levels that exist in the absence of the burst. These levels may be set by various causes:

(a) Receiver noise. This is generally not a problem on satellite experiments except with very short antennas.

(b) Spacecraft RFI. Conducted or radiated interference has been a problem with a number of spacecraft experiments and can greatly reduce the dynamic range and sensitivity of the experiment.

(c) Ionospheric and magnetospheric noise. At low frequencies the magnetosphere becomes a prolific source of various kinds of sporadic radio emission. At frequencies of several hundred kHz and below, magnetospheric noise often dominates the

background (Stone, 1973). This can be reduced only by going to large distances from the earth or behind the moon.*

(d) Galactic background. A large number of careful measurements have been made to determine the low-frequency galactic component (Alexander, 1971; Weber, 1972; Brown, 1973). This component drops rapidly with frequencies below several MHz.

The burst characteristics discussed here exhibit a strong dependence on frequency. These changes reflect the evolution of the burst exciter-plasma interaction as the exciter moves outward. The dependence of these parameters on frequency and other factors forms the basis for the detailed extraction of physical information described in part 3. However, at this point it is useful to give a first picture of this dependence over a wide range of frequencies for several important parameters.

---

*A spacecraft devoted to radio astronomy studies, RAE-2, has been launched successfully (June, 1973) into lunar orbit.

Figure 6 (Alvarez and Haddock, 1973) shows the wide range of drift rates characterizing type III bursts. It is striking that a power law dependence seems to hold over many decades. However, it is important to note that the scale of the figure can disguise many systematic variations present. For example, systematic drift rate changes which appear as small changes on this figure nevertheless contain very valuable information which can lead to a determination of emission levels (see part 3).

Figure 7 presents a similar overview of the variation of excitation time t_e and decay time t_d with frequency. Both parameters display a power law dependence on frequency with a similar slope and show that the type III profile scaled approximately as f^{-1} remains remarkably constant over a wide range of frequencies. However, there are systematic changes of these parameters (Aubier and Boischot, 1972) which are washed out on the scale of this figure.

Figure 8 (Evans et al., 1971) is an extension of a previous figure (Wild et al., 1963) with data from RAE-1 added. This indicates that the observed flux from both type III bursts and storms continues to increase with increasing wavelength. Figure 9 is a similar figure, giving brightness temperatures assuming a large emitting area for the low

frequency radiation (intersection of a 40^{o} cone with apex at the sun with the appropriate spherical plasma level).

3. ANALYSES OF RADIO BURST DATA

The analyses of solar radio bursts at low frequencies have proceeded in ways similar to earlier work done at higher frequencies. The goal is to account for the observable features of the bursts in terms of particle-plasma interactions and then to use the bursts to gain information about the complex processes and conditions existing in the solar environment. At lower frequencies where the exciter particles travel large distances,it is reasonable to expect that the bursts relate to large scale features of the solar wind.

In the following sections we summarize a number of analyses that have been made which have led to quantitative results. In many areas the field is evolving rapidly as new data and interpretations become available.

3.1 Emission Level Scale

The emission level scale of solar radio bursts is one of the more fundamental relations necessary to determine, since it relates directly to the interpretation of most

other burst parameters. Although the average emission level as a function of frequency is sought, it is clear that most observers realize that large scale fluctuations are likely because of the dynamic conditions in the outer corona. However, observations of the sizes of radio bursts and observations of the extent of energetic particles near 1 AU indicate that low-frequency solar burst regions subtend some tens of degrees from the sun so that any one burst is itself an average over a large region of space.

At higher frequencies, ground-based observers of solar bursts with large telescopes can measure the location of the emission levels directly, using limb events (Wild et al., 1963; Wild and Smerd, 1972). At frequencies below 80 MHz, refractive bending of ray paths through the ionosphere becomes increasingly important and large corrections must be made. For low-frequency observations made from space platforms above the ionosphere, the experiments so far have been restricted to antenna systems with dimensions short compared to wavelength so that sufficient direct antenna resolution is not possible.

In the following sections, analyses are reviewed which yield the emission levels of the observed solar radio bursts.

In order to relate the electromagnetic radiation to plasma density in the emission region it is necessary to know whether this radiation is observed at the fundamental or the harmonic of the source plasma frequency. When both the fundamental and harmonic components of solar bursts are observed, this identification is unambiguous. For type III bursts in the decametric and longer wavelength regions such pairs are very rare; it is not clear whether any single burst is observed at the fundamental or harmonic of the plasma frequency.

3.1.1 Drift rates

In the absence of position measurements, most observers have used the frequency drift in time of the radio bursts to get information on emission levels. The observed time that it takes a burst to drift from one frequency to a lower one depends on the distance separation between emission levels, the time it takes the exciter to pass between levels, and the difference in radio propagation time from each emission level to the observer.

In attempting to interpret dynamic spectra, one can assume that the exciter speed remains constant,

the trajectory radial or otherwise defined, and utilize the time difference between two heights to convert the drift rate observations to a distance scale. A comprehensive analysis of bursts observed with the Alouette satellites was carried out by Hartz (1969) in this manner for frequencies between 10 MHz and 0.6 MHz. He assumed an exciter speed of 0.35c and a level of 4.5 $R_{\odot}$ for the burst at 10 MHz and obtained results summarized in figure 10.

A somewhat different approach was followed also by Hartz (1969), as well as by Alexander et al., (1969) which was applicable to streamers of enhanced density. First, assuming collisional damping, the variation of electron temperature with frequency was obtained from the burst decay times. Then an equilibrium was assumed between the gas pressure plus magnetic pressure in the (assumed) streamer and the total pressure in the surrounding coronal plasma. Utilizing a model proposed by Sturrock and Smith (1968) in which a streamer is the visible manifestation of a current sheet between two tubes of opposite magnetic flux, the magnetic flux in the streamer wastaken to be negligibly small. Taking available models of density, temperature, and magnetic field

for the ambient solar wind, the temperature was found to decrease as R^{-1} and the density was enhanced by a factor of 10-20 as illustrated in figure 11 (Alexander et al., 1969). Realizing that the assumption of collisional damping might be in error, these authors investigated also the assumption that the temperature in the solar wind and streamer were similar. This model is designated as Model II. In this analysis, the observed radio emission is assumed to occur at the fundamental of the plasma frequency.

The opportunity to pursue a somewhat different analysis also based on drift rates occurred with RAE-1 satellite observations of a storm of type III bursts (Fainberg and Stone, 1970a,b, 1971a). This storm, consisting of many tens of thousands of bursts, was connected with the passage of one solar active region in August, 1968. Because of solar rotation, the radio emission travel time to the observer varied in a strikingly systematic way. Figure 12 shows the variation in observed peak drift times on a day-by-day basis through one half solar rotation. (The storm had also been visible in the previous solar rotation at a reduced intensity.) Using a least squares analysis

(Fainberg and Stone, 1971a), a function depending on three parameters(level separation, exciter speed, and time of central meridian crossing) was fitted to the data. In effect, this analysis utilized the change in observed burst characteristics due to the angular rotation of the sun, to compensate for the poor angular resolution of the dipole. Six frequencies from 0.54 MHz to 2.8 MHz was used and both the emission level separations and exciter drift rates were derived simultaneously corresponding to each pair of frequencies. With a level chosen for the radiation at 2.8 MHz, this analysis yielded an emission level scale with a power-law dependence on distance similar to the coronal density data summarized by Newkirk (1967). The least squares fit of the RAE data to a power law is given by

$$f_{obs} = 66.8\ R^{-1.315} \qquad (1)$$

where f_{obs} is observed type III burst frequency in MHz and R is distance to sun in solar radii, $R > 10\ R_{\odot}$. The RAE observations are shown in figure 10 and compared with other analyses based on single bursts.*

*An analysis based on intense burst groups observed on OGO-5 has been published recently (Alvarez and Haddock, 1973).

In order to derive densities at the corresponding emission levels, it is necessary to know whether the observed burst radiation is at the fundamental or the harmonic of the plasma frequency. The scale on the left in figure 10 is based on an assumption of fundamental radiation, and it is noted that such derived densities are an order of magnitude higher than estimates for the solar wind. Similar results obtained at higher frequencies have been interpreted in terms of emission taking place in dense streamers. However, the existence of large dense regions beyond 5 solar radii occurring often enough to account for type IIIs has not been reported. At 1 AU the in-situ measurements of density show enhancements by a factor of 10 to be very rare. If, however, the low-frequency type III radiation occurs at the harmonic of the plasma frequency, then derived densities from the observed emission levels are a factor of 4 lower and in better agreement with the Newkirk summary. This is indirect support for the interpretation that low-frequency type III solar bursts are observed at the harmonic of the plasma frequency. Further evidence for this is discussed later.

Additional information on emission levels is provided by determining the direction of arrival of radiation from limb events discussed in the next section and from an analysis of type II emission discussed in section 3.1.3.

3.1.2 Burst Arrival Direction

Due to antenna rotation on a spin-stabilized spacecraft, the received radiation possesses a definite modulation pattern. When the dipole axis is perpendicular to the source direction the received power is maximum; when the dipole axis is closest to the source direction the received power is minimum. It is clear that if the orientation of the antenna is known, then the direction of arrival of the radiation can be determined from the phase of the observed modulation pattern. In this manner Slysh (1967c) made estimates of the arrival direction of several bursts at 0.2 and 1 MHz. His results were apparently affected by limited information on spacecraft aspect.

This technique was developed to a high precision (Fainberg et al., 1972) with the experiments on IMP-6, launched in March, 1971. In this satellite, the spin axis was perpendicular to the ecliptic plane and

optical sensors were used to determined the sun position precisely. A powerful data-processing technique was developed at Goddard which utilized the entire modulation pattern to determine arrival directions. It was found possible to determine the burst arrival direction to within 1 degree accuracy with respect to the sun earth-line with just a few minutes of observed data. Figure 13 shows a type III burst originating near the solar west limb. The insert of this figure shows the spin modulation of the received signal for a portion of this burst at 250 kHz. From the modulation, burst arrival directions as a function of frequencies were determined and are shown in figure 14. The open circles on this figure indicate the points of closest approach of the burst arrival directions to the sun. The closed circles are the intersections of these lines with spherical emission levels based on the RAE emission level scale, eq (1). Figure 15 shows these data plotted on a density-distance scale. The lower line in this figure is an interpolated density scale between a value at 10 $R_{\odot}$ from light-scattering observations and a value at 1 AU from in-situ measurements. The open circles are the

distances of closest approach of the emission from the sun. The upper line is the RAE emission level scale if radiation occurs at the fundamental. If the radiation occurs at the harmonic, then the densities derived from the distance of closest approach become the set of squares. This limb event provides strong evidence that hecto-metric and kilometric bursts are observed at the harmonic of the plasma frequency. It is also significant that in many thousands of observed low-frequency type III bursts no cases have been reported by the Goddard group where both fundamental and harmonic components were observed.

Haddock and Alvarez (1973), however, have interpreted most complex type III events observed on OGO-5 as having fundamental and harmonic components. They have concluded that there is a transition frequency (which varies from burst to burst) below several MHz where the burst changes from predominantly fundamental to predominantly harmonic radiation. This interpretation depends on the appropriate identification of features of complex events measured with a radiometer with frequency separations of octaves. In the absence of published intensity-time profiles of any of the bursts used, it is not clear how unique such an identification

is. Moreover, ray tracing computations taking into account scattering and refraction suggest that for frequencies below 3 MHz it is very difficult for radiation near the plasma frequency to propagate out of the emission region, and when it does it may be delayed by many minutes from the harmonic radiation (Steinberg, 1973).

Upon examination of many type III bursts using 1-1/2 years of data from IMP-6, the Goddard group has found that the RAE emission level scale, eq. (1), is reasonable for levels out to 1 AU. At 1 AU, this scale indicates an emission level of 57 kHz. For a large number of bursts, spin modulation disappears near this frequency, implying that the spacecraft at 1 AU is surrounded by the emission region. In addition, the burst onset time of the 55 kHz channel most often corresponds to the onset of energetic electrons (Lin et al., 1973) measured on the same spacecraft as discussed in section 3.2.

3.1.3 Type II Observations

Additional support for the RAE scale and for the harmonic interpretation of type III bursts at low frequencies has been provided by the analysis of a low-

frequency type II shock event which occurred in Aug., 1973 (Malitson et al., 1973b). Such low-frequency type II events do show clearly identifiable fundamental and harmonic components (Malitson et al., 1973a) in strong contrast to low-frequency type III bursts where only one component is unambiguously observed. For this event, the initiation of the shock at the sun was well determined by the time of the associated flare and by high-frequency type II radio observations (Maxwell, 1973). The arrival of the shock at 1 AU was also well determined by the time of a large sudden-commencement magnetic storm. Figure 16 shows these observations on a distance-vs.-time plot, where the flare is represented by a dot in the upper left (around 1500 UT, 1 $R_{\odot}$). The sudden commencement geomagnetic storm is similarly represented by a dot at 2354 UT at 1 AU. The straight line drawn between them represents the average velocity of the shock front over the 1 AU distance, about 1270 km s^{-1}. Area A shows the observations of Maxwell (1973). Areas B,C, and D give the times during which type II radiation at the fundamental was being observed at the various frequencies from IMP-6. These observations have

been placed on figure 16 according to the RAE emission level scale, eq (1), i.e. assuming that the type III's are observed at the fundamental. If the alternate assumption is made that the type III's are observed at the plasma frequency harmonic, then the type II observations (at the fundamental) are plotted as in figure 17. In this case, some 30-kHz emission that was observed coming from the solar direction just before the arrival of the shock at the earth, is also plotted. The considerably better agreement of the IMP-6 data with the optical and magnetic observations seen in figure 17 suggests strongly that the RAE emission level scale refers to types III's observed at the harmonic of the plasma frequency.

3.2 Electron-Type III Correlations

The way in which energetic charged particles interact with a tenuous plasma to produce electromagnetic radiation is a fundamental question in radio astrophysics. The combination of low-frequency radio observations of solar bursts, and the in-situ measurements of the interplanetary plasma, magnetic field, and energetic solar particles affords a unique opportunity to study these processes within the source regions.

There now appear to be compelling reasons to believe that non-relativistic electrons with energies above 5 keV are the exciters of type III bursts, although protons and hydromagnetic shock waves have also been proposed in the past. Smith and Fung (1971) had considered protons as the exciter to overcome the theoretical difficulties associated with stabilization of a spatially unbounded and homogeneous electron stream. Proton events of the required energy of ~50 Mev are rare compared to the large number of type III bursts. Furthermore, proton events seem to correlate more closely with type II and IV solar bursts than with type III events.

Early studies revealed that solar electron events are almost always accompanied by type III bursts. These investigations were continued by Alvarez et al., (1972) who found an almost one-to-one correlation between intense kilometer wavelength type III bursts and $\gtrsim$ 20 keV electron events detected at 1 AU from flares located in the western solar hemisphere. As noted by these authors, the good correlation of hectometer type III with flares probably reflects the fact that only large radio bursts were used. Of a total of 56 distinct

type III bursts arising from flares, 26 that were located west of central meridian were followed about 25 minutes later by electron events observed at 1 AU. For type III bursts associated with flares located at longitudes east of W09, there were no correlations with electron events.

This type of solar longitude effect was understood in terms of the propagation characteristics of solar electrons along an Archimedean spiral field structure in the interplanetary medium. Electron events observed in the vicinity of the earth must travel along field lines which connect back to the sun in the vicinity of W50 solar longitude. Since these electrons cannot propagate easily across the magnetic field, Alvarez et al. attribute the wide solar longitude range observed to be due to the extended particle emission region of the order of 50^{o} at or near the sun.

A similar correlation exists between the hectometric storms discussed by Fainberg and Stone (1970a) and non-impulsive co-rotating $\geq$ 20 kev electron fluxes observed at 1 AU. Sakurai (1973) has investigated the occurrence of solar energetic particles and wide-band continuum storms

from metric to hectometric frequencies. Figure 18 illustrates the comparison of radio and electron data for one such period.

Results obtained by Frank and Gurnett (1972) and by Lin et al. (1973) provide further strong evidence that non-relativisitic electrons are the source of type III emission. However, the two papers disagree as to which energy electrons are involved. Frank and Gurnett interpret their results as implying that electrons of the order of 5-6 keV produce the radio emission while Lin et al. obtain results indicating electrons with energies in the range 10-100 keV are primarily responsible for the low-frequency emission.

In the Frank and Gurnett experiment, the radio emission onset time observed at 31 kHz was followed 2600 seconds later by the arrival of the 5-6 keV electrons. If these electrons are in fact the correct exciters, then the time delay would imply that the 31-kHz plasma level was located at a distance from the sun of less than 1 AU. The reason for their choice, made in the absence of positional information on source location, was that the local plasma density at 1 AU was 5.0 cm^{-3}, corresponding to a plasma frequency of the order of 20 kHz. Although the experiment had a channel

close to this frequency, no radiation was observed. The authors attribute this to the decreased burst intensity. With a plasma level of 20 kHz at 1 AU and assuming radiation at the fundamental of the plasma frequency only, the 31-kHz and higher-frequency plasma levels are established through an inverse-square-law dependence of density on distance. The time delay over this distance establishes the particle speed and thus an energy of 5-6 keV for the exciters.

The results of Lin et al., (1973) have the decided advantage of the directional information provided by the radio experiment. Furthermore, their analysis made use of the recent evidence that the radio emission occurs at the second harmonic of the plasma frequency. The solar electron events selected for analysis included a scatter-free event (27 April, 1972) and one exhibiting a diffusive time profile (16 May, 1971). The trajectory of the May 1971 event as determined by the radio observations is shown in Figure 19. Assuming that the burst is centered on the ecliptic plane, the angular size of the 67-kHz radio burst viewed from the spacecraft is about 160^{o} which would require it to be located at about 190 $R_{\odot}$. At the observing

frequency of 55 kHz, the absence of spin modulation indicates that the burst is isotropic and therefore requires this level to be essentially at the satellite's orbit (1 AU). Since the radiation occurs at the second harmonic, a frequency of 55 kHz is consistent with an average solar wind density of 4-8 cm^{-3} (Wolfe, 1972) at 1 AU. The arrival times at 1 AU of electrons of various energies are compared with the radio observations in Figure 20 for the May 1971 and April 1972 events over the frequency range from 2600 to 44 kHz.

Although burst profiles frequently appear simple at the lower frequencies, they may in fact be compound as can be seen for these cases at the higher frequencies. This somewhat typical characteristic complicates analysis over a large range of frequencies and leads to some degree of uncertainty in measurements of drift rates, particularly at the higher frequencies. In figure 20, O and M refer respectively to the onset and maximum of the bursts at the lower frequencies. The arrival times of electrons of various energies are also indicated on the figure. For Figure 20a, the 55-kHz emission onset time is coincident

with the arrival of the 100-200 keV electrons. The burst grows to its maximum intensity as the more numerous lower-energy electrons arrive. For this diffuse electron event, particle observations give a total trajectory length L of 1.68 AU while the radio observations (Figure 19) give an L of 1.25. The apparent path difference is explained in terms of pitch angle scattering of the burst exciter. This is also consistent with the difference between drift velocities derived from the radio data and the speeds of the corresponding particles.

The scatter-free event of April 1972 reveals that in this case the emission frequency of 44 kHz occurs near 1 AU. The onset of the radio burst at this frequency again corresponds to the arrival of 100-200 keV electrons. For this event, L is found to be 1.4 AU from electron onset times compared to 1.25 AU from the radio data. This suggests that since there is less scattering, there sould be a larger drift rate derived from the radio data. The drift rate is found to be a factor of 2 greater here than for the May 1971 diffuse event.

Therefore, the picture which evolves from the analysis of Lin et al. (1973) is that electrons with energies of

~10-100 keV are the exciters of type III bursts. The two events, observed under conditions of differing plasma density at 1 AU, lead to the same result. For both events the burst maximum corresponds to the arrival of ~10 keV electrons while the start of the constant decay phase of the burst (indicating end of excitation) occurs with the arrival of electrons of energy of the order of 5-6 keV.

The results of Frank and Gurnett (1972), as they point out, would yield 24 keV as the energy of the associated electrons if the radio burst (6 April 1971) was observed at the second harmonic. This interpretation seems compelling since the directions of arrival of the radio emission (determined by the GSFC experiment on IMP-6 for the 6 April 1971 event) place the emission at least a factor of 2 farther out from the sun than the positions used by Frank and Gurnett. In addition, the higher sensitivity of the GSFC radio exeriment indicates somewhat earlier onset times for the low-frequency radio burst components, bringing the burst at 1 AU into better agreement in time with the $>$ 45-keV electron channel.

The view provided by these analyses of electron events is that electrons associated with type III bursts are

emitted at the sun with an abrupt onset and with fluxes having a power law (differential) dependence on energy from several hundred keV to below several keV. On travelling out from their source region the electrons develop a separation of energies near the leading edge. It appears that during this separation significant radio burst excitation occurs (Lin et al., 1973).

The density of fast particles at the time of maximum intensity of the 55-kHz radio emission is $\sim 10^{-6}$ cm^{-3} for the May 1971 event. An estimated source size, from higher frequency observations, of $\sim 40^{o}$ fWHM and the receiver bandwidth give a volume of $\sim 8 \times 10^{37}$ cm^{3} containing 8×10^{31} fast electrons. From the maximum emission of 8.8×10^{-11} $ergs/cm^{2}$ sec at 55 MHz, Lin et al. estimate that the loss rate to electromagnetic radiation is small and of the order of 4×10^{-9} keV/sec per fast electron.

3.3 Burst Trajectory

The locus of the type III burst emission region in space is the path of the exciter particles. Because of the small gyroradii of these particles, they are constrained to move out along the large-scale magnetic field lines. In

this way, the radio observations of type III bursts can provide unique information on magnetic field configurations in the solar wind.

3.3.1 Solar Storm Studies

In the analysis of the hectometric storm of August 1968 (Fainberg and Stone, 1971a) it was found that there was a progressive delay with increase in altitude, in the time of CMP of the emission region as solar rotation carried it westward. Sakurai (1971) investigated the associated flare and type I activity (Nancay) during this period and showed that there were present two large active regions (McMath 9593 and 9597) separated by about 30^{o} in longitude. Both the hectometric noise storm and the type I noise storm seemed to be associated with the latter region (9597). On the other hand, Stewart and Labrum (1972) found that the 80-MHz positions of the type III bursts observed at Culgoora were displaced to the west of the type I storm region. They point out that these locations indicate that the type I activity was located in a region of strong loop-type magnetic fields, while the type III storm (with high-frequency cutoffs) started in the weak-field regions, probably near a magnetic cusp. In this view, strong MHD

waves propagating through the type I source region to the cusp region trigger pinch instabilities leading to electron accelerations at relatively high points in the corona.

3.3.2 U Bursts

The dynamic spectra of U bursts are characterized by a drift to lower frequencies and a subsequent return drift to higher frequencies. The initial drift rate is similar to that of type III bursts, but decreases as the reversing frequency f_{min} is approached. U bursts, which are not rare at meter wavelengths, are considered to be a variant of type III events in which the exciter is constrained after the initial outward motion to return to lower coronal heights along a magnetic loop structure produced, for example, by a bipolar field configuration.

The occurrence of low-frequency U bursts is rare, although ten such events have been clearly identified in the analysis of several years of RAE-1 data near solar maximum. One U burst observed at hectometer wavelengths by the RAE-1 satellite is shown in figure 21a (Stone and Fainberg, 1971). Assuming a constant exciter speed of

0.3c and combining this with two constraints—the radial distance scale and the total distance along the path upward from a particular plasma level and back down to the same level-the trajectory shown in figure 21b was obtained. Using the RAE-1 density scale with the reversing frequency, the outer extent of the magnetic loop was found to be about 35 $R_{\odot}$. Schatten (1968) has indicated that magnetic loops convected outward which lead to new magnetic sectors are not rare.

3.3.3 Individual Burst Events

Low-frequency burst measurements of intensity and arrival direction combined with an emission level scale allow a determination to be made of the radio trajectory through interplanetary space for events such as is illustrated in figure 19. This figure, however, is a summary over the history of the event; it is of considerable interest to examine the dynamic processes during the passage of individual type III bursts. A computer technique for processing IMP-6 data to show the dynamic nature of the bursts was developed at Goddard. The format of the plots is shown in figure 22. The plane of the figure is the ecliptic with west to the

right and east to the left. A grid of four concentric circles separated by 50 $R_\odot$ is plotted. A fifth innermost circle is located at 5 $R_\odot$; the way in which satellite measurements complement ground-based observations can be appreciated by noting that ground-based measurements deal primarily with phenomena occurring within the 5 $R_\odot$ circle.

For each minute of spin-modulated data, the arrival direction is determined. The intersection of this direction with the level given by the emission level scale is determined and a radial line segment is plotted with a length proportional to the logarithm of the burst intensity above background. Figure 22 consists of a collection of these intersections for a period of 5 minutes. The plot shows a solar burst in progress with the main part of the burst located at 50 $R_\odot$. If the start time of each frame is advanced a small amount, a movie can be prepared which graphically presents the progress of the burst moving out from the sun. Figure 23 shows a sequence of frames separated by 2 minutes during this radio burst. These are taken from a movie shown at IAU Symposium No. 57 on Coronal Disturbances (Surfer's Paradise, Australia, 1973). For an extended period of days

before and after this burst, there was a low-level solar storm of thousands of type III bursts detectable out to 1/3 AU. At 2026 UT, the larger type III burst is just visible near the sun. At later times, the radio emission regions of interplanetary space farther out become visible. At 2036 UT the main part of the exciter is located between 50 and 100 $R_\odot$, but the faster particles have moved ahead and have reached 1 AU. From this frame, the Archimedean spiral of the interplanetary magnetic field guiding the burst exciter is evident. At later times, the excitation at higher frequencies ceases and by 2050 UT the burst for the first 100 $R_\odot$ is no longer visible; the activity present in that region is that of the long-lasting solar storm. This particular burst had a faster than usual frequency drift rate.

Some bursts exhibit cutoffs at one end or the other of their range. In figure 24 a type III burst starts at 1531 UT near 50 $R_\odot$ and progresses outward to 1 AU. At 1602 UT a second burst starts much closer to the sun and progresses along much of the same trajectory. The first event is an unusual extreme case of a class of bursts that

exhibit high-frequency cutoffs. Often such bursts are western limb events, so that the cutoff is probably caused by EM wave refractive effects. This case, however, may be an example of electron acceleration due to reconnection of magnetic fields very distant from the solar surface. In other cases, low-frequency cutoffs exist. Figure 25 shows two bursts which fade out before reaching 50 $R_\odot$. Other bursts were observed that exhibit kinks and reverse curvature in their trajectories. It is clear that a range of interplanetary phenomena remain to be explored by these radio techniques.

3.4 Burst Exciter Properties

The properties of the burst exciter will be better understood when more is known about the physics of the very complex beam-plasma-electromagnetic-wave interaction processes. Although many theoretical investigations have been made (see Smith, 1973), the theory of how much electromagnetic radiation is produced by a given charged particle beam moving through interplanetary space is not yet at the stage of yielding reliable results.

In the absence of complete theoretical treatments, some investigators have tried to draw physical interpretations about the exciter properties based on very crude simplifying assumptions. Such assumptions can be criticized in many ways, but, nevertheless, it is often of interest to see where they do lead.

The starting place for some of these studies (Hughes and Harkness, 1963; Aubier and Boischot, 1972; Evans et al., 1973) are the observed intensity-time profiles of the radio burst at various frequencies. The basic idea here is that the rise portion of the radio burst is directly related to the buildup of plasma oscillations in the medium as the exciter moves through a particular coronal level; the longer decay phase of the burst is related to the decay of the plasma oscillations through various possible damping mechanisms. The frequency drift of the burst in time reflects the velocity of the exciters as they move outward. The growth in the burst rise time at lower frequencies, in this view, reflects the growth in the physical length of the exciter because of its velocity dispersion.

In this manner Aubier and Boischot (1972) related the intensity of the radio burst I(t) at time t to the exciter profile P(t'), where t' is the time measured from the start of the exciter when at the coronal level corresponding to the observing frequency.

Then

$$I(t) = \int_{o}^{t} P(t')\, e^{-\frac{(t-t')}{t_d}}\, dt' \qquad (2)$$

where t_d is the e-folding decay time.

If the exciter has a duration in time of t_e, then

$$I(t) = (\text{constant})\, e^{-t/t_d}, \text{ for } t > t_e. \qquad (3)$$

By plotting the burst profile on a ln(I) vs. time plot, as in figure 5, t_e and t_d can be determined for simple bursts. The top part of figure 5 shows a burst profile measured on 19 June 1971 at 155 kHz while the lower curve gives the same data with the cosmic noise continuum background subtracted. The time t* is the effective time at which the burst profile clearly changes to exponential decay, and with the subtraction of the onset time yields the excitation time t_e.

Figure 5 shows clearly the commonly observed exponential decay typical of type III bursts. In this case the exponential decay extends uniformly over four decades of intensity. Single large bursts permitting this analysis are rare and usually account for less then several percent of bursts observed. However, it usually appears that groups of bursts are composed of overlapping single bursts with similar characteristics.

Evans et al., (1973) have analyzed 35 single bursts observed with RAE-1 and IMP-6 covering the frequency range of 2.8 to 0.067 MHz, which corresponds to emission levels from 10 $R_\odot$ to 200 $R_\odot$. They find that this range of data (from 2.8 MHz to 0.067 MHz) exhibit a power law dependence on frequency with least squares fits given by

$$t_e = 4.0 \times 10^8 \ f^{-1.08} \qquad (4)$$

$$t_d = 2.0 \times 10^8 \ f^{-1.09} \qquad (5)$$

where f is in MHz, and t_d and t_e are in seconds. These results as well as results in the literature obtained by other workers are shown in figure 7. Both quantities show a frequency dependence which varies approximately as f^{-1}

over a wide range of frequencies. Since t_e is a measure of the burst rise and t_d is a measure of the burst decay, this dependence on frequency indicates that the type III burst profile normalized by f^{-1} is remarkably constant over a large frequency range.

3.4.1 Exciter Velocity

Values of exciter speed are usually derived from drift-time measurements in conjunction with an emission level scale. Satellite measurements over the first 40 $R_\odot$ (Hartz, 1969; Fainberg and Stone, 1970b) have yielded average exciter speeds of about $c/3$ and indicate that there is no appreciable slowdown over that range. However, an analysis of IMP-6 data (Fainberg et al., 1972) yielded a measurable slowdown apparent at greater distances. Figure 26 shows this result. Similar results exist for other bursts (Evans, 1973).

These results do not necessarily imply a loss of energy in the exciter stream corresponding to the velocity change. It may be that increased pitch angles along the path due to scattering reduce the projected forward velocity without appreciably affecting the energy. Evidence that the total path traveled by electrons is longer than the average

spiral distance to the sun has been reported by (see Lin, 1973). In addition, Lin also reports that electrons are measured with appreciable pitch angles at 1 AU.

Investigators have tended to think of the exciter particles in terms of a packet of superthermal particles with a small spread of velocities. The small spread is required by the observed rate of growth of the burst rise time at increased distances. The restricted range of velocities in such an exciter leads to difficulties because of the rapid slowdown via the two-stream instability, as pointed out by Sturrock (1964). Various investigations have been undertaken to see what effects might stabilize such a velocity distribution with much recent work available (see Smith, 1973).

Observations of energetic electrons measured simultaneously with radio bursts at low frequencies have been discussed in section 3.2; there, evidence was presented that the accelerated packets of electrons near the sun have a power law distribution of energies with more electrons at lower energies, at least down to several keV. In such an electron stream, energy loss to plasma waves is very slow because the coherent

effects related to a positive slope on the distribution function are not present. This is true, except that with an abrupt stream onset the faster electrons move out ahead of the slower ones, leading to the possibility of coherent energy loss at the leading edge of the stream (Baldwin, 1964; Zaitsev et al.,1972). The observations of Lin et al.,(1973) show that at 1 AU such a velocity separation does occur, leading to an observed positive slope on the differential energy spectrum which moves down to lower energies at later times. The electron radio burst comparisons (Lin et al., 1973) in figure 20 show that the radio burst excitation occurs at the leading edge of the stream during the passage of the first electrons possessing energies of several hundred keV down to ~10 keV. It is clear that much detailed work on these processes remains (Zaitsev et al., 1972). Recent work on nonlinear stabilization of the electron beam applicable to the leading edge looks promising (Popadopoulos et al., 1973).

Until a complete analysis is available it is not immediately clear which energy electrons are most effective. For instance, close in to the sun near the beginning of the

event the faster-moving electrons may be most important; farther out, where the velocity separation has had more time to disperse the exciter, the more numerous slower electrons may be more effective in producing radio waves, leading to an apparent exciter slowdown.

3.4.2 Exciter Length

Assuming that the radiation bandwidth is small, the length of the excitation region passing a given level in the corona can be estimated from the product of the burst excitation time t_e with the average exciter speed (Hughes and Harkness, 1963). Using the variation in exciter speed with distance taken from figure 26, the radial size L of the excitation region at distance R was found (Evans et al., 1973) to be:

$$L = 170\ R_\odot \text{ at } R = 190\ R_\odot \quad (67\ \text{kHz})$$

$$L = 16\ R_\odot \text{ at } R = 24\ R_\odot \quad (1\ \text{MHz}).$$

Aubier and Boischot (1972) by a similar analysis at higher frequencies found

$$L = 0.9\ R_\odot \text{ at } R = 1.5\ R_\odot \quad (36.9\ \text{MHz}).$$

Thus the exciter extent amounts to a large fraction of the source distance from the sun.

3.4.3 Exciter Velocity Dispersion

To investigate the effects of velocity dispersion $\Delta V/V$ of the exciter, a model of the change of exciter length with distance is required. Because of the inherent uncertainties involved in such theoretical calculations as well as in the observations, Evans et al., (1973) have adopted a simple two-stage model, which reflects the two distinct regions in which the exciter propagates. Close to the sun where the solar magnetic field is the dominant influence, the model of Weiss and Wild (1964) for propagation along or near a neutral sheet has been used. For distances larger than 10-20$R_\odot$, the magnetic field is carried out with the expanding plasma. The transition point between field-and flow-dominated motion was assumed to be 10 $R_\odot$.

The injection condition was taken by these authors as isotropic over a vertical hemisphere with a velocity distribution given by

$$F(v) = \exp\left[-\frac{(v-v_o)^2}{2\sigma^2}\right] \qquad (6)$$

where v_o = constant and σ = velocity dispersion.

Above 10 $R_\odot$ a simple expansion model was employed to investigate the growth of the particle packet. Using this two-stage model, Evans et al., (1973) have calculated values of t_e for three values of velocity dispersion, $\Delta v/v$ = 0.2, 0.39 and 0.75 ($\Delta v = 2\sigma$). The results of these calculations were compared with observed values of t_e not only at low frequencies but also with those quoted in the literature at higher frequencies (e.g. Weiss and Sheridan, 1962; Elgaroy, 1965; Aubier and Boischot, 1972). If it is assumed that the exciter velocity is constant, the comparison of observations with calculations suggests an apparent increase in velocity dispersion of the packet with increasing distance from the sun. In fact, this apparent increase is evident throughout the entire frequency range, covering both regions of propagation.

However, this apparent increase in dispersion can also be interpreted as a relative slowdown of the majority of the particles with respect to the leading edge. Therefore, utilizing the decrease of exciter speed from figure 26, the theoretical and experimental values of t_e obtained are shown in figure 27. The low-frequency observations are seen to be

consistent with a constant dispersion of ≈ 0.39 provided that the exciter speed decreased with distance from the sun as determined by Fainberg et al. (1972). The high-frequency observations can also be made consistent with this dispersion if the injection angular volume is made smaller, i.e. into a 45^{o} half-angle cone instead of into a hemisphere. This is shown by the dashed curve in figure 27.

3.4.4 Burst Decay

The exponential decay of type III bursts has been observed in single bursts to remain constant over 5 decades of intensity. This has great significance because it suggests a damping process with an energy loss proportional to the energy remaining. In addition, it implies that the damping constant t_d is not a function of either time or intensity and furthermore that the conversion efficiency from plasma waves to radio emission must also not be dependent on intensity or time. The possibility of the time and intensity dependence exactly balancing each other to give the observed decay seems unlikely.

At the present time, the physical process responsible for the decay of type III radio bursts is not

understood. Several mechanisms which have been suggested for the burst decay are Landau damping and collisional damping.

In collisional damping (Jaeger and Westfield, 1949) it is assumed that the observed decay of the type III bursts is due to the damping of plasma oscillations via Coulomb electron-ion interactions. In this case the damping time for Coulomb electron-proton collisions is given by (Spitzer, 1962)

$$t_d = 2.0 \times 10^6 f^{-2} T_e^{3/2} \qquad (7)$$

where T_e is the electron temperature and f the frequency in Hz.

Thus from the observed decay times the coronal electron temperature T_e can be determined. Application of this technique at high frequencies has led to derived temperatures which are in reasonable agreement with coronal conditions (Kundu, 1965). However, recent work by Aubier and Boischot (1972) at decametric frequencies based on this technique has yielded larger temperature gradients at longer wavelengths than seem reasonable. In addition, the low-frequency measurements of t_d have yielded a temperature fall-off with distance

from the sun that increases the discrepancy (Hartz, 1964; Slysh, 1967c; Hartz, 1969; Alexander et al., 1969; Haddock and Graedel, 1970) to the extent that T_e derived in this manner is well over an order of magnitude too low at 1 AU (Evans et al., 1973).

Solar wind observations of electron and proton temperatures have yielded an average temperature ratio smaller than predicted, and calculations have been made based on increased non-collisional coupling effects (Wolff etal., 1971). Alvarez and Haddock (1973) have shown that the radial dependence of this suggested enhanced coupling is nearly equal to that required by the radio observations to account for the observed burst decay times.

Other explanations of the radio burst damping have been suggested which are based on Landau damping processes. Zaitsev et al. (1972) have considered Landau damping of the plasma waves by exciter electrons after the leading edge has passed. They give burst profiles calculated in a one-dimensional treatment of this process which seem to agree well with small hectometric bursts. However, the agreement is not good for large bursts where the theoretical profiles

fall off much too rapidly and do not yield the 4-5 decade region of exponential decay observed in large bursts. Harvey and Aubier (1973) have considered the effects of Landau damping caused by the density decrease in the source region resulting from the outward convection of the solar wind. This density decrease causes the phase velocity of plasma waves to reduce to the point where Landau damping from the medium becomes dominant. However, the calculations of Harvey and Aubier (1973) indicate that an abrupt turnoff of the radio burst at low frequencies should occur shortly after the burst peak and this is not observed. It may be that some of the plasma waves can escape this fate by propagating towards the sun to compensate for the outward convection.

4. CONCLUDING REMARKS

The analyses of satellite observations of type III solar radio bursts made thus far have shown their great potential for the study of interplanetary processes.

More results can be expected from currently available data, on the relation of type III burst trajectories to large-scale features of the solar wind, including magnetic sector structure and plasma density inhomogeneities such

as coronal holes as well as coronal transient effects following large flares. The effects of scattering (Steinberg et al., 1971) on observed source directions and sizes must be considered in more detail. Additional radio burst comparisons with energetic particle events can be expected to provide new quantitative information about the beam-plasma interactions.

The recently launched lunar orbiting radio astronomy spacecraft, RAE-2, will provide additional information about source directions and sizes derived from occultation studies of radio bursts. A joint NASA-GSFC and Meudon Observatory radio satellite experiment utilizing a spinning tilted dipole antenna pattern which will permit the two-angle tracking of radio bursts is planned for a 1978 launch. This experiment will yield the first results on the gross features of the interplanetary magnetic field configurations out of the ecliptic. The value of this experiment would be greatly enhanced by two spacecraft able to make simultaneous observations from an extended baseline. Source location could be determined by triangulation and this would determine the 3-dimensional trajectories of the bursts through the

interplanetary medium without the use of models of average radio emission levels. The radio experiment on the HELIOS satellite (1974 launch) which will have a solar orbit as close as 1/3 AU should bring significant new information on the basic emission and propagation processes. Direct measurement of plasma waves may be possible with this spacecraft when the antennas are in the burst excitation regions.

We may anticipate that the combination of radio observations and particle measurements will stimulate a successful theoretical treatment of the emission process. Besides the contribution to radio astrophysics in general, a comprehensive picture of the emission process combined with electromagnetic observations over a wide spectrum will culminate in a more detailed picture of interplanetary processes and dynamic conditions at the electron acceleration region itself.

ACKNOWLEDGEMENTS

The authors wish to thank Harriet H. Malitson, Larry G. Evans, and Richard Fitzenreiter for their invaluable help in the preparation of this paper and to Peggy Wilson for preparation of the manuscript.

REFERENCES

Alexander, J.K.,:1971, in F. Labrum and R. Lust (eds.), New Techniques in Space Astronomy, IAU Symp. 41, 401.

Alexander, J.K., Malitson, H.H., and Stone, R.G.: 1969, Solar Phys. 8, 388.

Alvarez, H. and Haddock, F.T.: 1973, Solar Phys. 29, 197.

Alvarez, H. and Haddock, F.T.: 1973, in R. Ramaty and R.G. Stone (eds.), High Energy Phenomena on the Sun Symposium Proceedings, Preprint X-693-73-193, Goddard Space Flight Center, Greenbelt.

Alvarez, H., Haddock, F.T., and Lin, R.P.: 1972, Solar Phys. 26, 468.

Aubier, M. and Boischot, A.: 1972, Astron. Astrophys. 19, 343.

Baldwin, D.E.:1964, Phys. Lett. 12, 202.

Boischot, A.: 1967, Ann. Astrophys. 30, No. 1, 85.

Brown, L.W.: 1973, Astrophys. J. 180, 359.

Dunckel, N., Helliwell, R.A., and Vesecky, J.: 1972, Solar Phys. 25, 197.

Elgaroy, O.: 1965, in J. Aarons (ed.), Solar System Radio Astronomy, Plenum, New York.

Elgaroy, O., and Lyngstad, E.: 1972, Astron. & Astrophys. 16, 1.

Evans, L.G.: 1973, private communication.

Evans, L.G., Fainberg, J., and Stone, R.G.: 1971, Solar Phys. 21, 198.

Evans, L.G., Fainberg, J., and Stone, R.G.: 1973, Solar Phys., in press.

Fainberg, J., Evans, L.G. and Stone, R.G.: 1972, Science 178, 743.

Fainberg, J. and Stone, R.G.: 1970a, Solar Phys. 15, 222.

Fainberg, J. and Stone, R.G.: 1970b, Solar Phys. 15, 433.

Fainberg, J. and Stone, R.G.: 1971a, Solar Phys. 17, 392.

Fainberg, J. and Stone, R.G.: 1971b, Astrophys. J. 164, L123.

Frank, L.A. and Gurnett, D.A.: 1972, Solar Phys. 27, 446.

Haddock, F.T., and Alvarez, H.: 1973, Solar Phys. 29, 183.

Haddock, F.T. and Graedel, T.E.: 1970, Astrophys. J. 160, 293.

Hakura, Y, Nishizaka, R., and Tao, K.: 1969, J. Radio Res. Labs. Japan 16, 215.

Hartz, T.R.: 1964, Ann. Astrophys. 27, 831.

Hartz, T.R.: 1969, Planet. Space Sci. 17, 267.

Harvey, C.C. and Aubier, M.G.: 1973, Astron. Astrophys. 22, 1.

Hughes, M.P. and Harkness, R.L.: 1963, Astrophys. J. 138, 239.

Jaeger, J.C. and Westfold, K.C.: 1949, Austral. J. Sci. Res. A2, 322.

Kellogg, P.J., Lai, J.C., and Cartwright, D.G.: 1973, World Data Center A UAG-28, Part II, Boulder, 288.

Kundu, M.R.: 1965, Solar Radio Astronomy, New York, Interscience.

Lin, R.P.: 1973, Space Sci. Rev., this issue.

Lin, R.P., Evans, L.G., and Fainberg, J.: 1973, Astrophys. Lett. 14, 191.

Malitson, H.H., Fainberg, J., and Stone, R.G.: 1973a, Astrophys Lett. 14, 111.

Malitson, H.H., Fainberg, J., and Stone, R.G.: 1973b, Astrophys J. 183, L35.

Maxwell, A.: 1973, private communication.

Maxwell, A., Howard III, W.E., and Garmire, G.: 1960, J. Geophys. Res. 65, 3581.

Newkirk, G., Jr.: 1967, Ann. Rev. Astron. Astrophys. 5, 213.

Popadopoulos, K., Goldstein, M.L. and Smith, R.A.: 1973, submitted to Astrophys. J.

Rosenberg, H., De Groot, T.,: 1973, Space Sci. Rev., this issue.

Sakurai, K.: 1971, Solar Phys. 16, 125.

Sakurai, K.: 1973, Planet. Space Sci. 21, 17.

Schatten, K.H.: 1968, Ph.D. Thesis, Univ. of Cal., Berkeley.

Sheridan, K.V., and Attwood, C.F.: 1962, Observatory, 82, 155.

Slysh, V.I.: 1967a, Astron. Zh. 44, 94, Sov. Astron., AJ 11, 72.

Slysh, V.I.: 1967b, Astron. Zh. 44, 487, Sov. Astron., AJ 11, 389.

Slysh, V.I.: 1967c, Kosm. Issled, 5, 897; Cosm. Res. 5, 759.

Smith, D.F.: 1973, Space Sci. Rev., this issue.

Smith, D.F. and Fung, P.C.W.: 1971, J. Plasma Phys. 5, 1.

Spitzer, L.: 1962, Physics of Fully Ionized Gases, Interscience, New York.

Steinberg, J.L.: 1973, Private communication.

Steinberg, J.L., Aubier-Giraud, M., Leblanc, Y., and Boischot, A.: 1971, Astron. Astrophys. 10, 362.

Stewart, R.T., and Labrum, N.R.: 1972, Solar Phys. 27, 192.

Stone, R.G.: 1973, Space Sci. Rev. 14, 534.

Stone, R.G. and Fainberg, J.: 1971, Solar Phys. 20, 106.

Stone, R.G., and Fainberg, J.: 1973, in R. Ramaty and R.G. Stone (eds.), High Energy Phenomena on the Sun Symposium Proceedings, Preprint X-693-73-193, Goddard Space Flight Center, Greenbelt.

Stone, R.G., Malitson, H.H., Alexander, J.K., and Somerlock, C.R.: 1968, in K.O. Kiepenheuer (ed.), Structure and Development of Solar Active Regions, D. Reidel, Dordrecht, 585.

Sturrock, P.A.: 1964, in W.N. Hess (ed.), Physics of Solar Flares, AAS-NASA Symp., Washington, NASA SP-50.

Sturrock, P.A. and Smith, S.M.: 1968, Solar Phys. 5, 87.

Weber, R.R.: 1972, Astrophys. J. 177, 707.

Weber, R.R., Alexander, J.K. and Stone, R.G.: 1971, Radio Sci. 6, 1085.

Weiss, A.A., and Sheridan, K.V.: 1962, J. Phys. Soc. Japan Supp. A-II 17, 223.

Weiss, A.A. and Wild, J.P.: 1964, Austral J. Phys. 17, 282.

Wild, J.P., and Smerd, S.F.: 1972, Ann. Rev. Astr. Astrophys. 10, 159.

Wild, J.P., Smerd, S.F., and Weiss, A.A.: 1963, Ann. Rev. Astr. Astrophys. 1, 291.

Wolfe, J.H.: 1972; in C.P. Sonnett, P.J. Coleman, Jr., and J.M. Wilcox (eds.), Solar Wind, NASA SP-308, Washington.

Wolff, C.F., Brandt, J.C. and Southwick, R.G.: 1971, Astrophys. J. 165, 18.

Young, C.W., Spencer, C.L., Moreton, G.E., and Roberts, J.A.: 1961, Astrophys. J. 133, 243.

Zaitsev, V.V., Mityakov, N.A. and Rapoport, V.O.: 1972, Solar Phys. 24, 444.

FIGURE CAPTIONS

1. Dynamic spectra of type III bursts at hectometer wavelengths observed with the RAE-1 satellite. The upper figure shows computer-developed dynamic spectra from 5.4 to 0.3 MHz with 1-db intensity contours. The lower figure shows the intensity profiles at six frequencies corresponding to the horizontal lines through the upper figure. A single type III burst is shown in figure (a) illustrate typical rise, decay and drift times in this part of the spectrum. Figure (b) illustrates the complex structure resulting from the merging of groups of single events.

2. A 30-min segment of data of a solar storm of type III bursts near CMP. The drift in frequency, limited burst bandwidth, and large numbers of small bursts can be seen.

3. A 30-min segment of data from the same storm as figure 2 but 4 days prior to CMP. The lower occurrence rate and slower drift rate of the bursts is evident.

4. The minimum (left) and average (right) flux for 10-min periods of the August, 1968 storm as a function of heliographic longitude (day number) of the associated active region. The temporary decrease in storm activity on August 21 was also observed at metric frequencies. The average flux consists of both continuum and burst components, while the minimum flux at the higher frequencies is essentially the continuum component.

5. Intensity-time profile of a typical single burst. The upper figure represents the burst envelope with spin modulation removed by computer processing. The lower plot has the background removed and exponential decay extending over 4 decades of intensity. The excitation time is t_e.

6. Typical frequency drift rates (from Alvarez and Haddock, 1973) of type III bursts over a wide range of frequencies.

7. Typical decay times (left scale) and excitation times (right scale) of type III bursts over a wide range of frequencies.

8. The energy flux spectra of various components of solar radio emission. The high-frequency curves are from Wild et al. (1963). The RAE-1 data for the December, 1968 burst should be considered as lower limits as the receivers were saturated by the burst.

9. The brightness-temperature spectra of various components of solar radio emission. The high-frequency curves are from Wild et al., (1963). The RAE-1 data for the December, 1968 burst should be considered as lower limits as the receivers were saturated by the burst.

10. Electron density vs. distance from the sun in the outer corona. The solid curve represents the values given by Newkirk (1967) as best estimates during solar minimum. The values given by the radio measurements are from single bursts and are placed assuming the type III radiation was observed at the fundamental of the local plasma frequency. They should be displaced downward a factor of 4 if the radiation was observed at twice the plasma frequency.

11. Models of the variation of electron density and temperature with distance (Alexander et al., 1969) from the center of the sun for the "average" corona and for active region streamers. Model I streamer temperatures are derived from burst decay times; Model II streamer and "average" temperatures are assumed to be equal. The circled points represent streamer temperature derived from decay times reported by Malville (1962) at 25 MHz and streamer density found by Malitson and Erickson (1966) at 26.3 MHz.

12. The dependence of burst drift rate between 1.3 and 1.0 MHz on heliographic longitude for the August, 1968 storm. The least squares fit, indicated by black circles in the figure, gives a level separation of 4.4 $R_{\odot}$ and an average exciter speed of 0.35 c.

13. A type III burst observed between 1 MHz and 30 kHz by the IMP-6 radio experiment. The insert figure illustrates the observed spin modulation at a frequency of 250 kHz, while for the main figure, only the burst envelopes are shown for clarity.

14. Directions of arrival (in the ecliptic plane) determined from the spin modulation for the burst in figure 13. The trajectory shown by the black dots is fixed by using the RAE-1 emission level scale (see text). The trajectory shown by the open circles is determined by the distance of closest approach permitted by the arrival direction.

15. Interplanetary density and plasma frequency scale as a function of distance in solar radii. The interpolated density scale is given by a line between the value determined by light-scattering observations, labeled L, and that from space probe measurements, labeled S. The circles are the density scale corresponding to the closest approach trajectory shown in Figure 14, assuming radiation occurs at the plasma frequency. These points map into the squares if radiation occurs at the second harmonic of the plasma frequency.

16. Comparison of observations from IMP-6 of a type II solar radio burst with the average velocity of the shock front, assuming that the type III bursts used to derive coronal emission levels were observed at the plasma frequency (Malitson et al., 1973b)

17. Same as fig. 16 except for the assumption that the type III bursts were observed at the second harmonic of the plasma frequency, and the inclusion of the 30-kHz data.

18. The time variation of solar radio continuum emission in metric and hectometric frequencies (200, 2·8 and 1·31 MHz) and of solar keV electrons ($\geq$ 22 and $\geq$ 45 keV ranges).

19. Average trajectory of a type III burst for which simultaneous electron measurements were made. See figure 19.

20. (a) Intensity-time profiles (spin modulation removed) of a type III burst observed on 16 May 1971 for frequencies from 2600 kHz to 44 kHz. The loss of spin modulation at 55 kHz places this level at 1 AU. Note the observed electron onset times.
(b) The burst of 27 April, 1972. In this case the loss of spin modulation places the 44-kHz level closest to 1 AU. (Lin et al., 1973).

21. (a) Dynamic spectrum of a hectometer U burst. Numbers on the figure indicate intensity in decibels relative

to cosmic noise background. Note the frequency limit of the return branch. (b) The magnetic bottle inferred from the U burst. The model is based on the RAE-1 density scale (see text) and an assumed exciter speed of 0.3 c. Bars on the figure show the positions determined from the dynamic spectrum relative to the start of the burst.

22. Format of a computer-generated plot of data from IMP-6. The plane of the figure is the ecliptic with the IMP-6 and Earth located at bottom - ⊕. For each minute of data, the intersection of the measured type III arrival directions with the spherical emission level is determined, and a radial line segment with length proportional to log intensity is plotted. This figure is a collection of data from 32 frequencies spaced taken at 5 sec intervals for a 2-min period.

23. Frames separated by 2-min intervals during a large type III burst. A low-level solar storm visible over the first 1/3 AU is present before and after the burst.

24. Two type III bursts. The first, starting near 1531 UT, shows no high-frequency components although it was quite large. The second burst starting near 1602 UT, does have high-frequency components.

25. Two type III bursts with no low-frequency components.

26. Average burst exciter velocity(v) divided by the velocity of light (c), as a function of distance from the sun for the trajectory of closest approach. Corrections were made for the travel time of light. The burst onset times yielded the values labeled by triangles and correspond to the faster particles in the exciter. The burst peak times yielded the values labeled by X and correspond to particles producing most of the radio burst energy. These results are based on the analysis of only one burst, that shown in Figure 13.

27. Calculated curves and observational values of t_e vs. frequency. The calculated curves were obtained assuming the exciter velocity decreases with distance, for distances greater than 10 $R_\odot$. The solid curves assume the injection conditions are into a vertical hemisphere. The dashed curves are for injection into a smaller volume, approximately a 45^o half-angle cone.

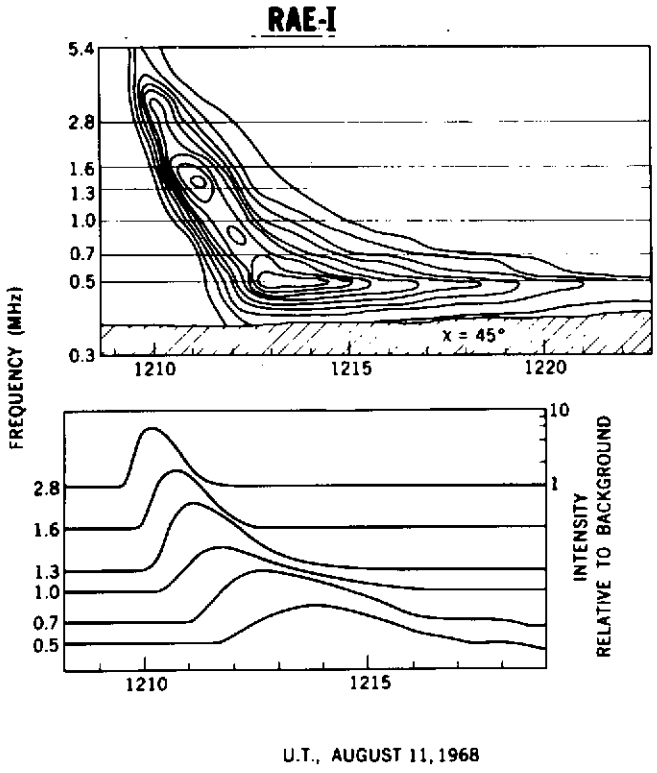
RAE-I
FREQUENCY (MHz)
5.4
2.8
1.6
1.3
1.0
0.7
0.5
0.3
χ = 45°
1210
1215
1220
10
1
INTENSITY
RELATIVE TO BACKGROUND
U.T., AUGUST 11, 1968

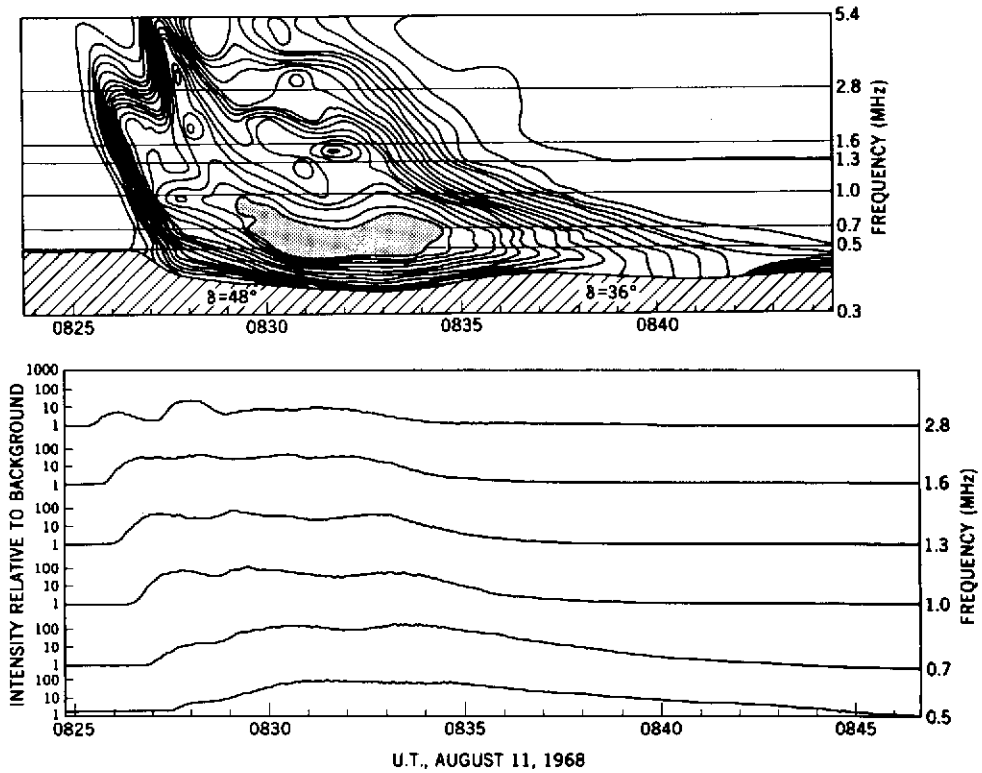
δ=48°
δ=36°
0825
0830
0835
0840
0845
INTENSITY RELATIVE TO BACKGROUND
FREQUENCY (MHz)
U.T., AUGUST 11, 1968

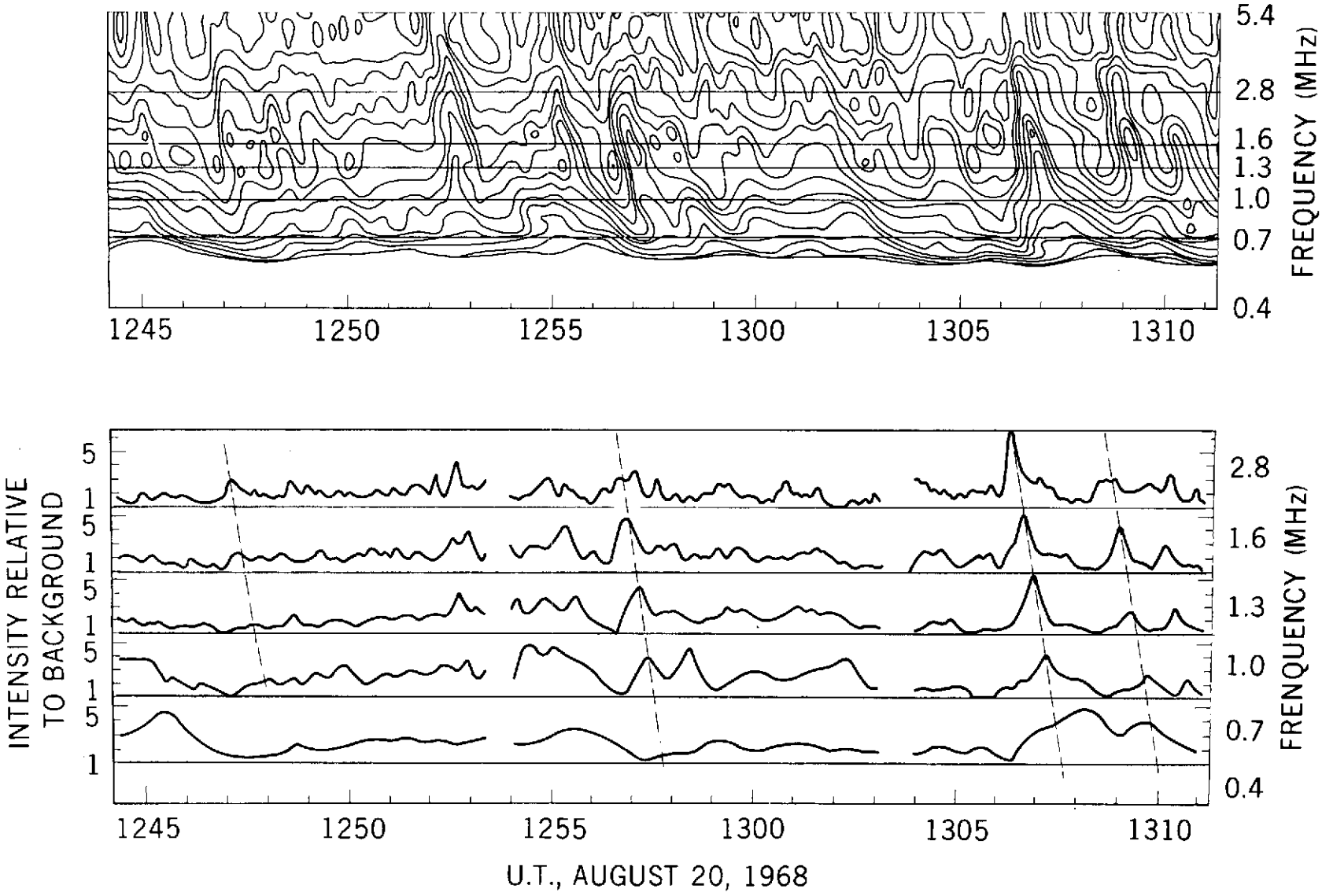
5.4
2.8
1.6
1.3
1.0
0.7
0.4
FREQUENCY (MHz)
1245
1250
1255
1300
1305
1310
INTENSITY RELATIVE TO BACKGROUND
5
1
2.8
1.6
1.3
1.0
0.7
0.4
FRENQUENCY (MHz)
U.T., AUGUST 20, 1968

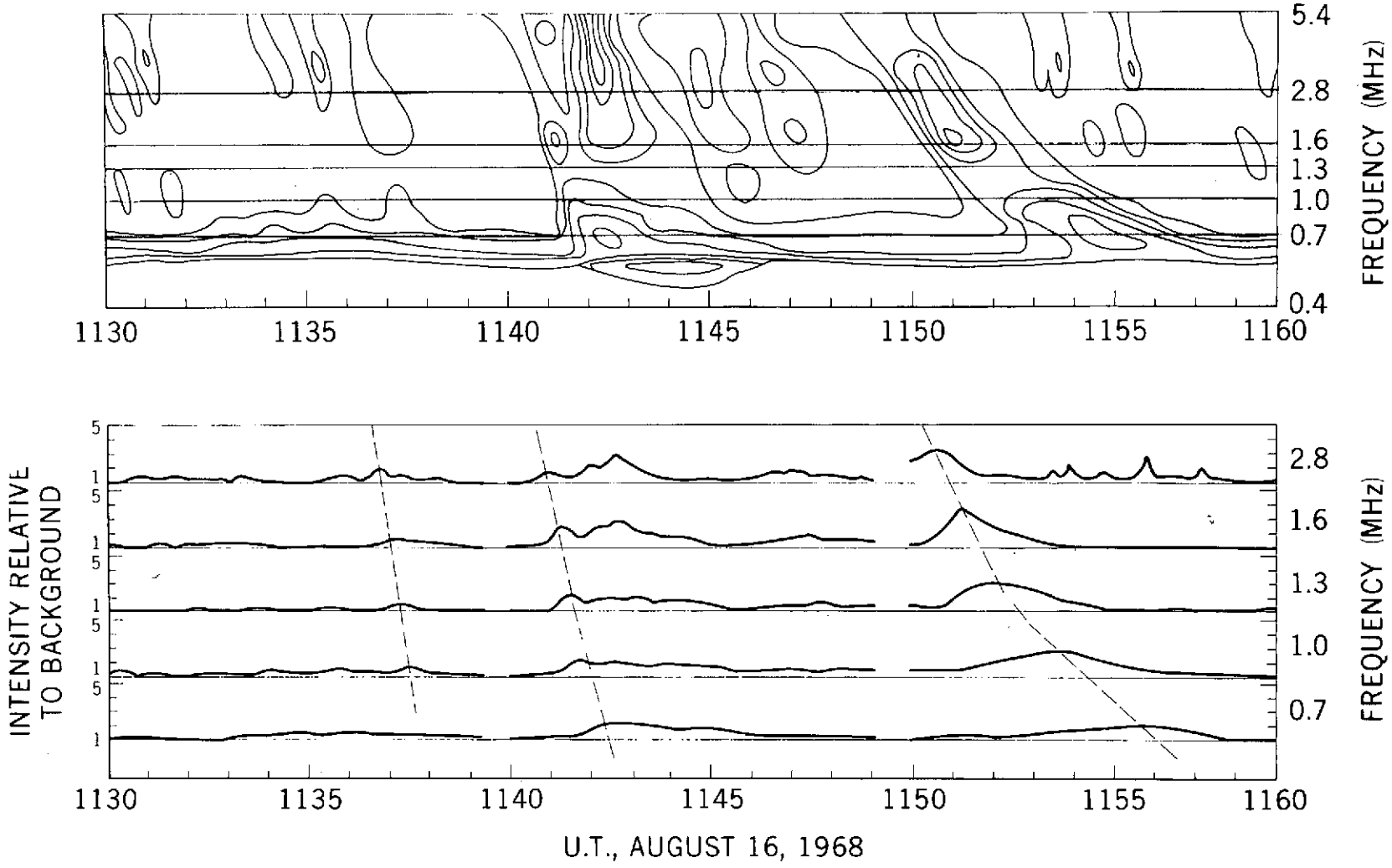
5.4
2.8
1.6
1.3
1.0
0.7
0.4
FREQUENCY (MHz)
1130
1135
1140
1145
1150
1155
1160
INTENSITY RELATIVE TO BACKGROUND
5
1
5
1
5
1
5
1
5
1
2.8
1.6
1.3
1.0
0.7
FREQUENCY (MHz)
1130
1135
1140
1145
1150
1155
1160
U.T., AUGUST 16, 1968

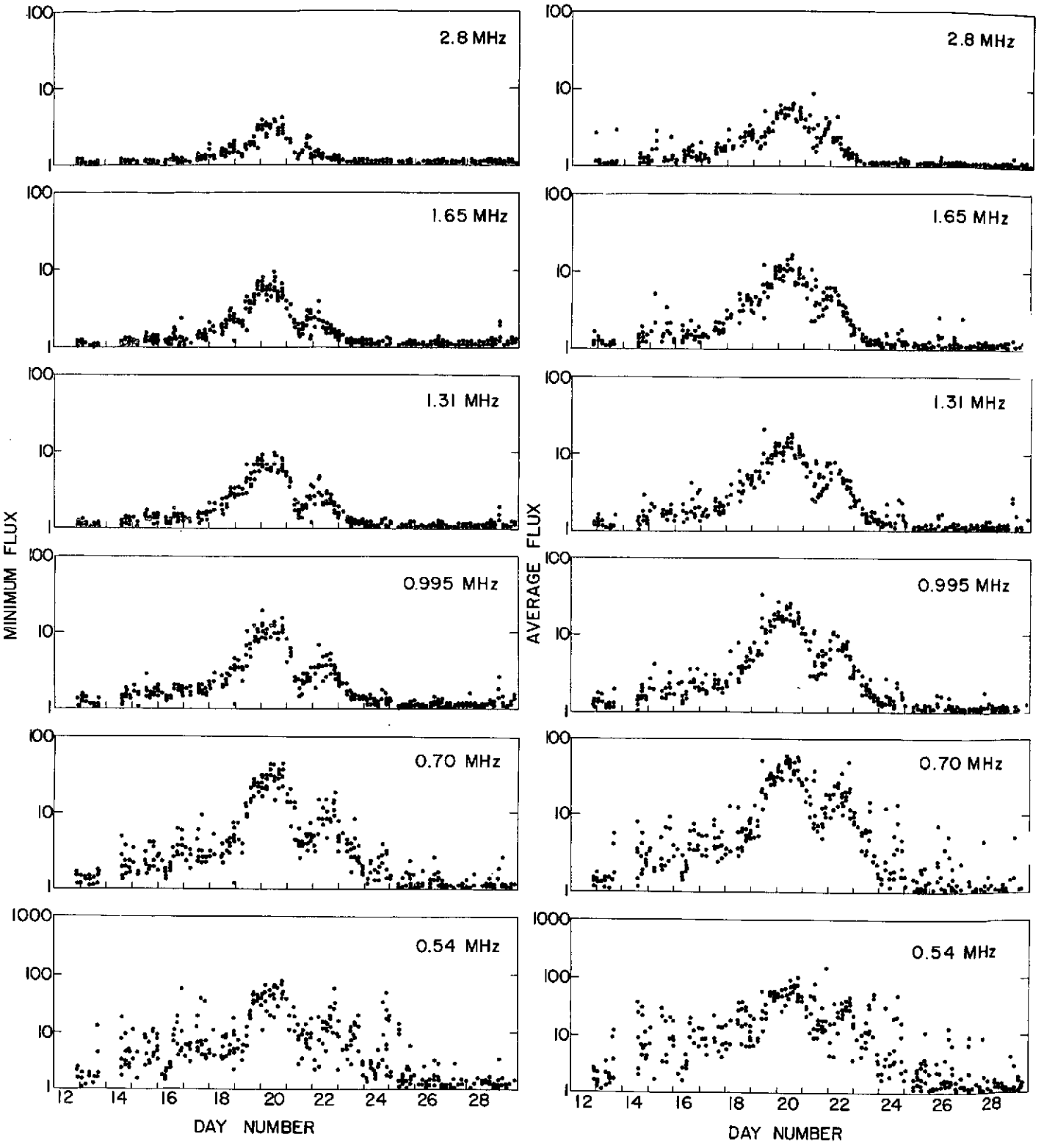
2.8 MHz
1.65 MHz
1.31 MHz
0.995 MHz
0.70 MHz
0.54 MHz
100
10
1
1000
MINIMUM FLUX
AVERAGE FLUX
12
14
16
18
20
22
24
26
28
DAY NUMBER

AUGUST 1968

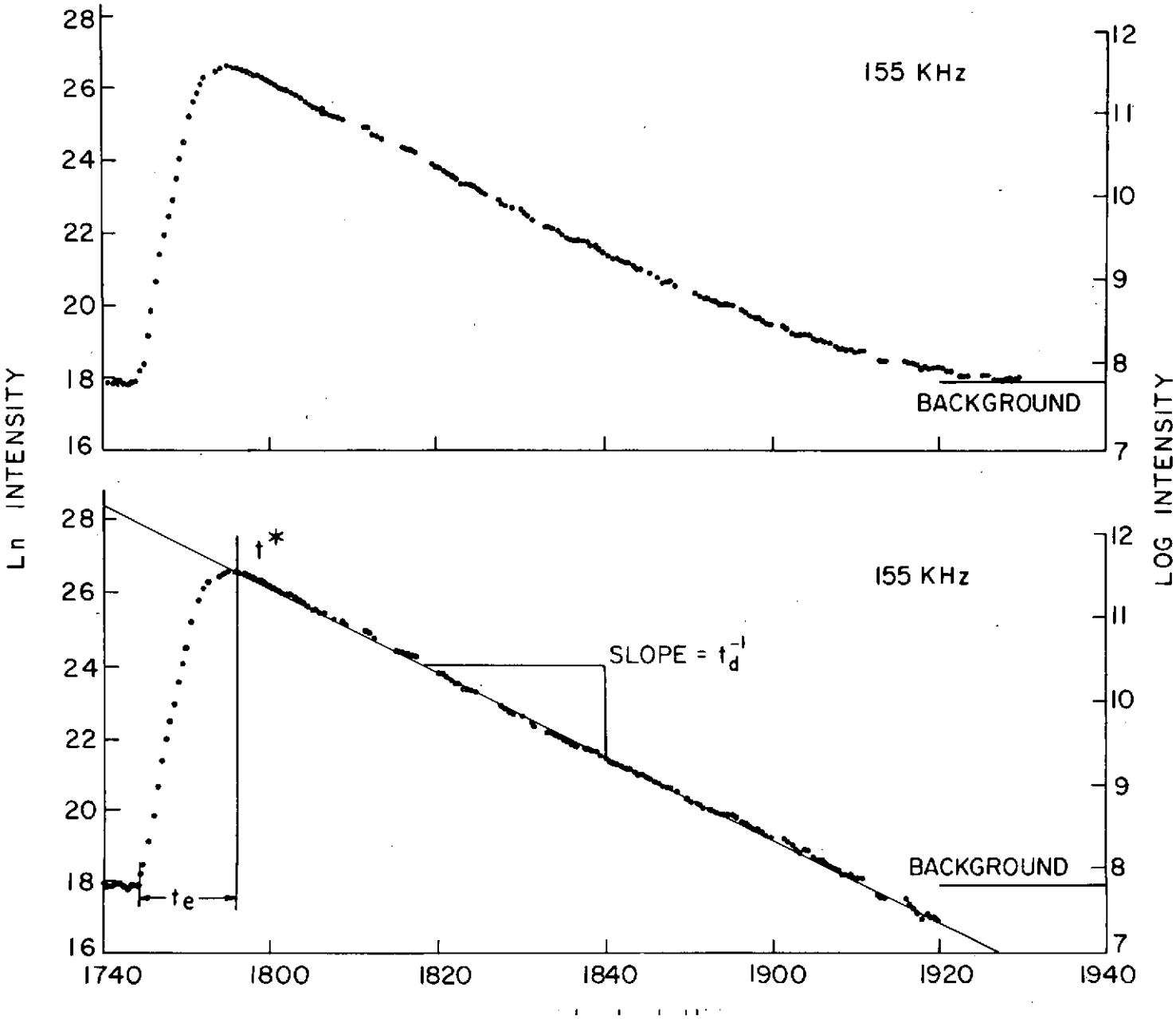
155 KHz
BACKGROUND
Ln INTENSITY
LOG INTENSITY
t*
SLOPE = t_d^{-1}
t_e
28
26
24
22
20
18
16
12
11
10
9
8
7
1740
1800
1820
1840
1900
1920
1940

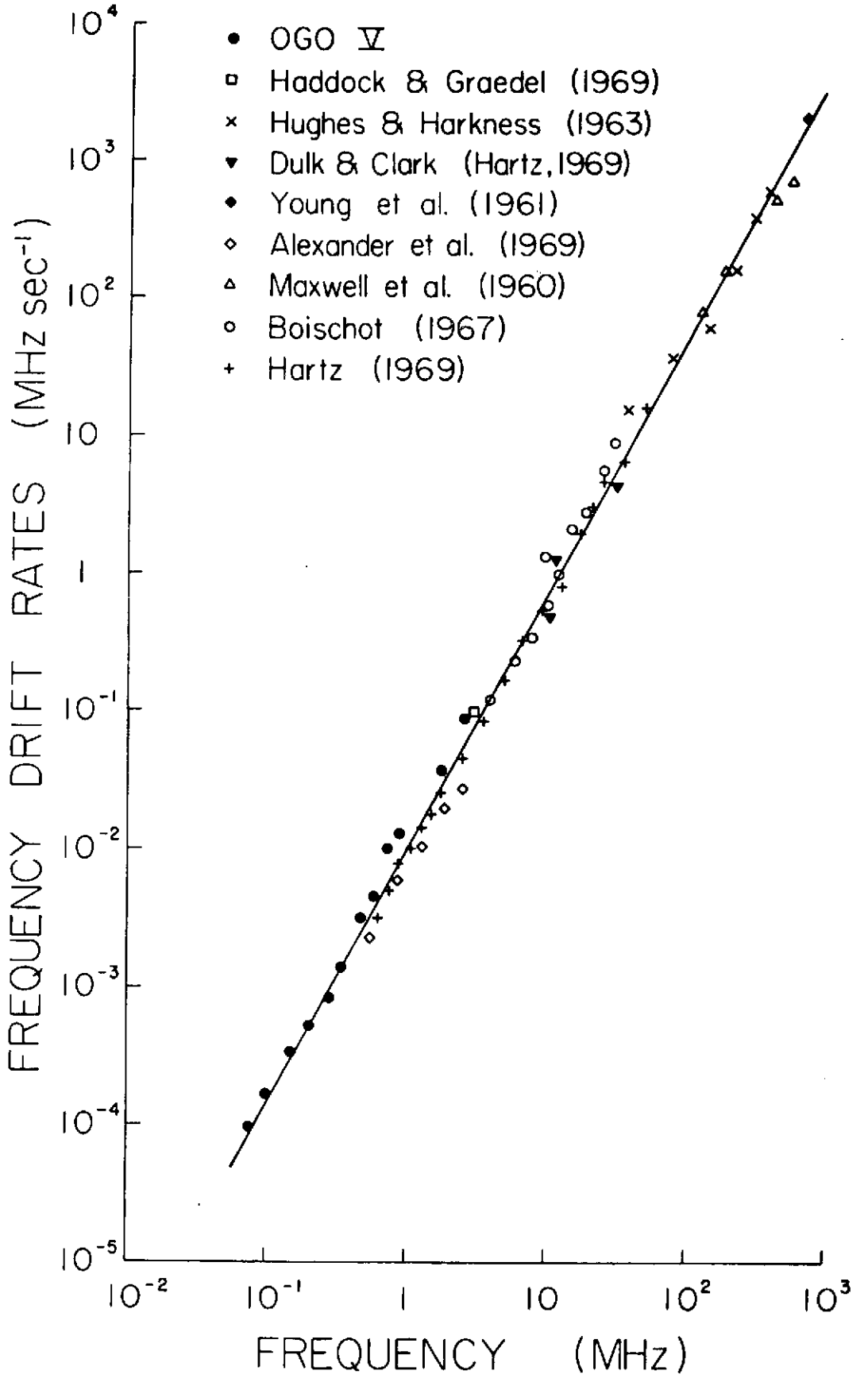

FIG. 4.5 FREQUENCY DRIFT RATES FOR TYPE III BURSTS.

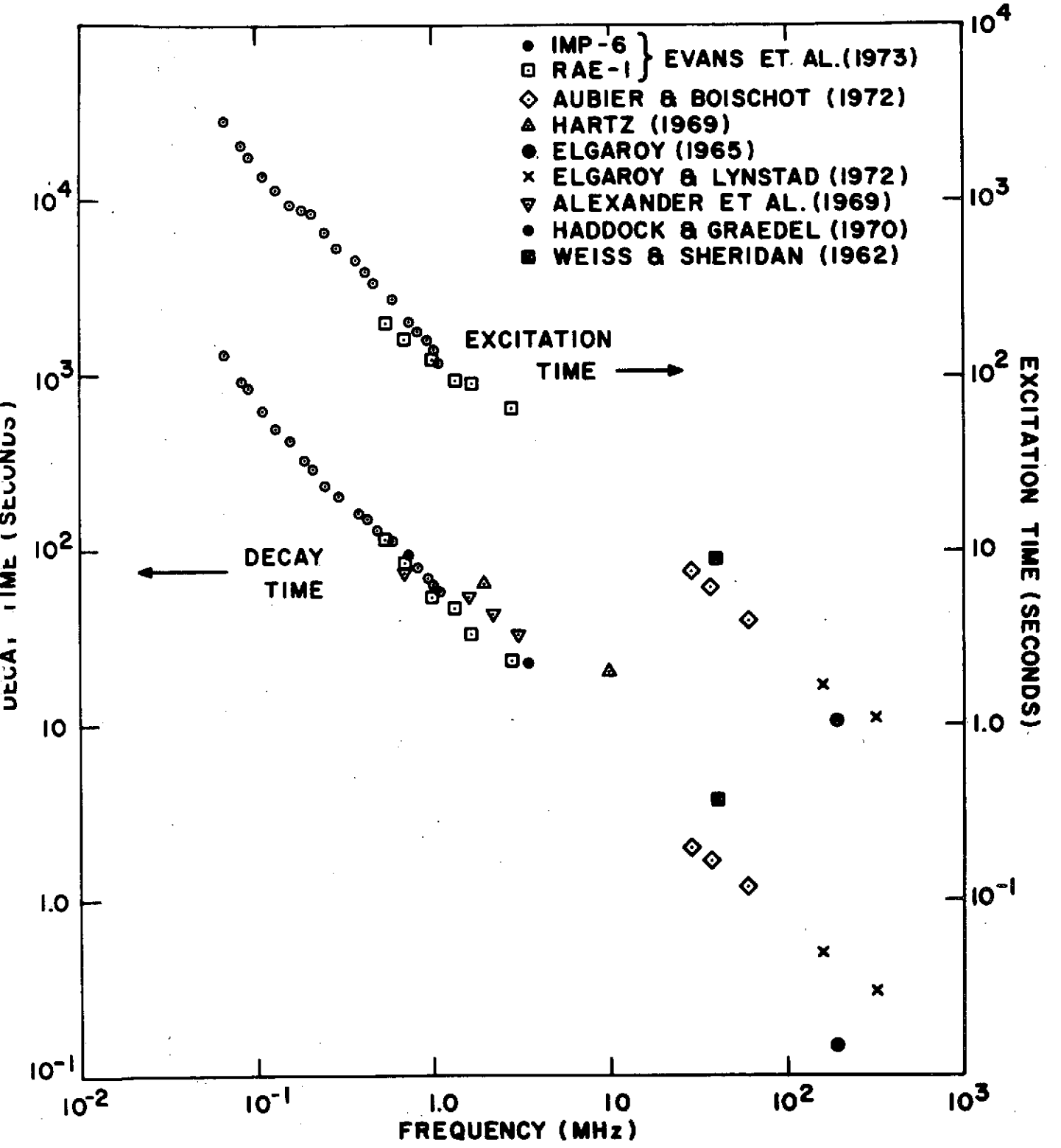
IMP-6
RAE-1
EVANS ET AL.(1973)
AUBIER & BOISCHOT (1972)
HARTZ (1969)
ELGAROY (1965)
ELGAROY & LYNSTAD (1972)
ALEXANDER ET AL.(1969)
HADDOCK & GRAEDEL (1970)
WEISS & SHERIDAN (1962)
EXCITATION TIME
DECAY TIME
DECAY TIME (SECONDS)
EXCITATION TIME (SECONDS)
FREQUENCY (MHz)
10^4
10^3
10^2
10
1.0
10^-1
10^-2

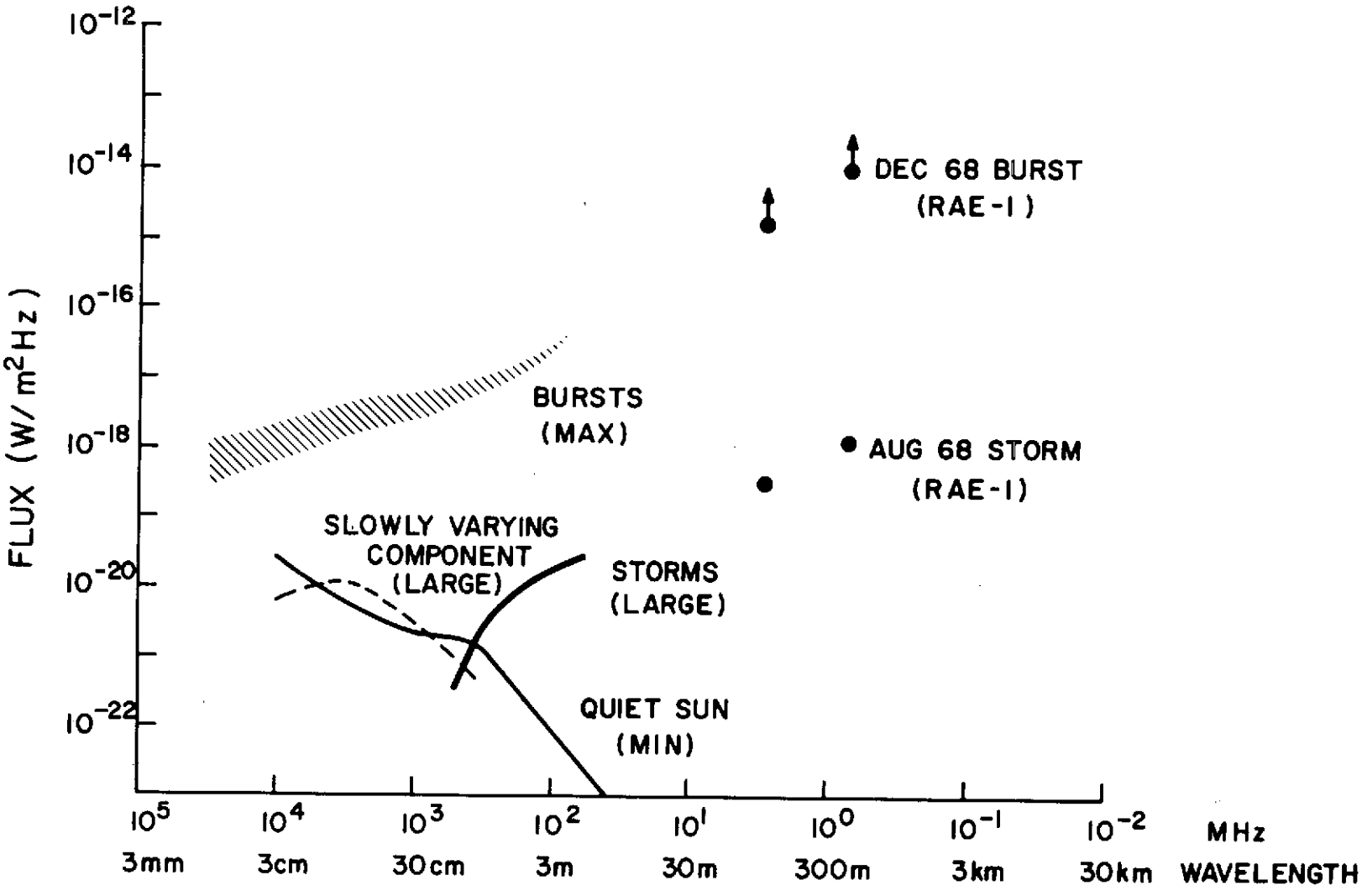
FLUX (W/m²Hz)
10⁻¹²
10⁻¹⁴
10⁻¹⁶
10⁻¹⁸
10⁻²⁰
10⁻²²
DEC 68 BURST
(RAE-1)
AUG 68 STORM
(RAE-1)
BURSTS
(MAX)
SLOWLY VARYING
COMPONENT
(LARGE)
STORMS
(LARGE)
QUIET SUN
(MIN)
10⁵ 10⁴ 10³ 10² 10¹ 10⁰ 10⁻¹ 10⁻²
MHz
3mm 3cm 30cm 3m 30m 300m 3km 30km
WAVELENGTH

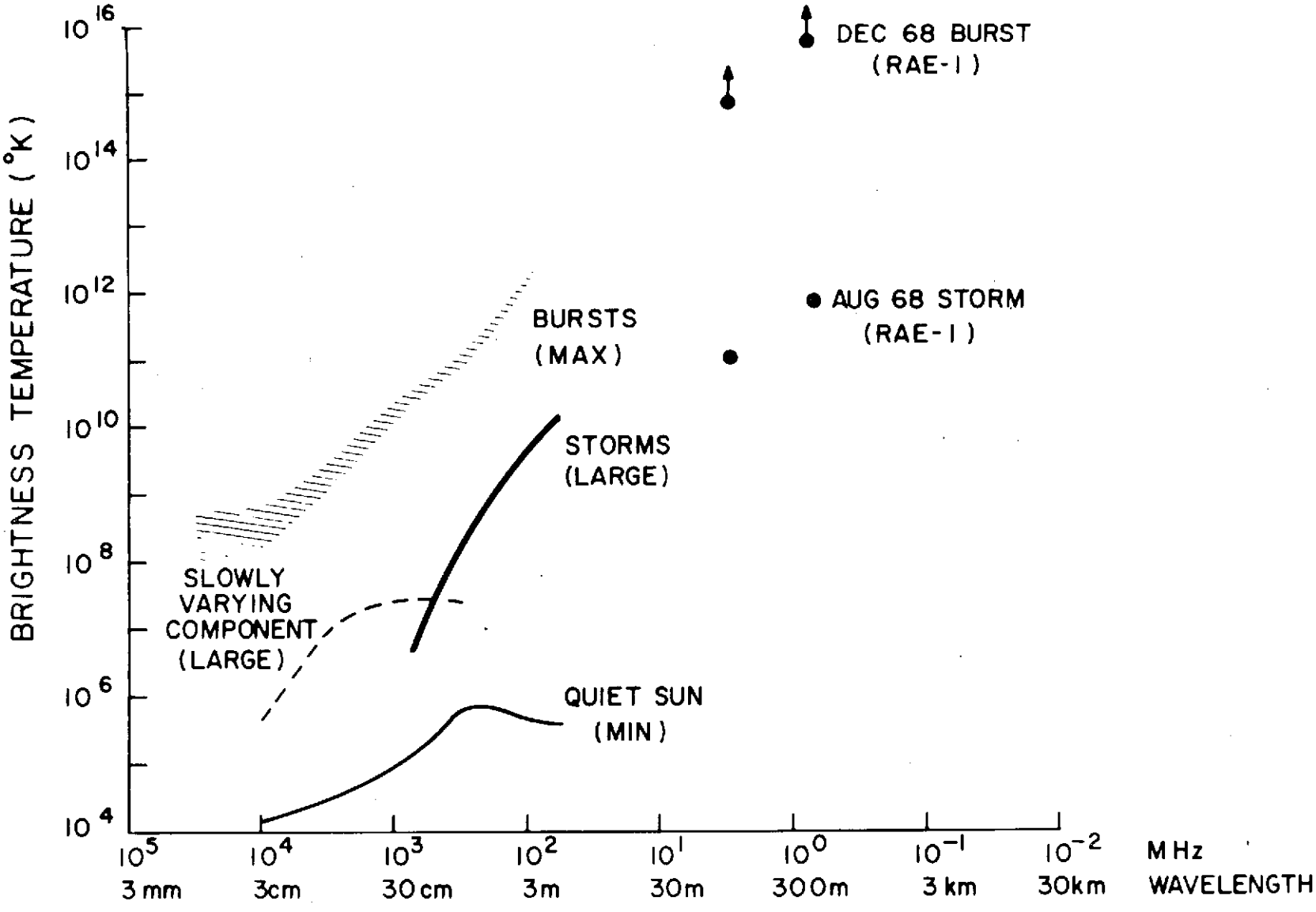
BRIGHTNESS TEMPERATURE (°K)
10^16
10^14
10^12
10^10
10^8
10^6
10^4
DEC 68 BURST
(RAE-1)
AUG 68 STORM
(RAE-1)
BURSTS
(MAX)
STORMS
(LARGE)
SLOWLY
VARYING
COMPONENT
(LARGE)
QUIET SUN
(MIN)
10^5
3 mm
10^4
3cm
10^3
30 cm
10^2
3m
10^1
30m
10^0
300m
10^-1
3 km
10^-2
30km
MHz
WAVELENGTH

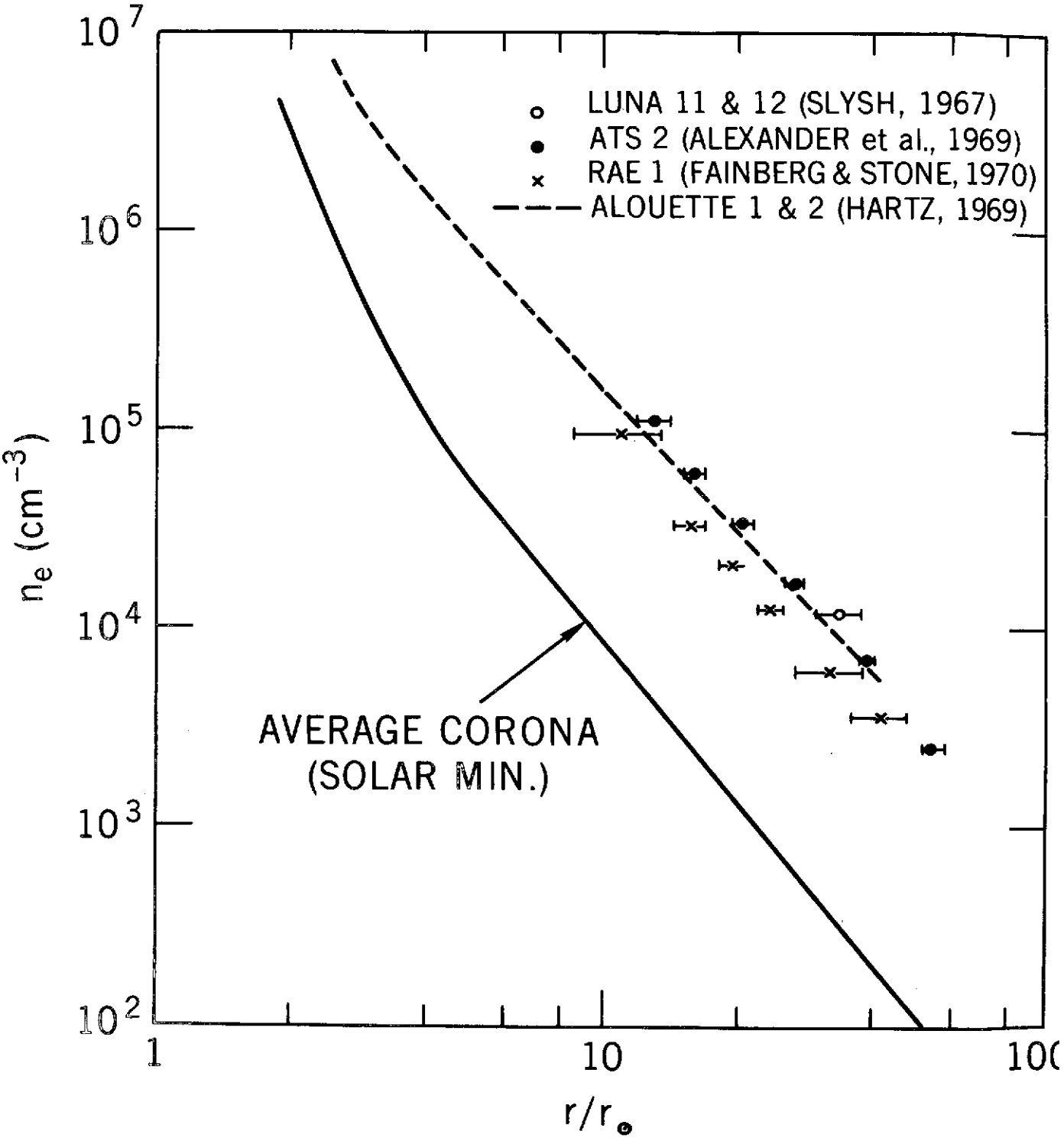
10^7
10^6
10^5
10^4
10^3
10^2
n_e (cm^{-3})
1
10
100
$r/r_\odot$
LUNA 11 & 12 (SLYSH, 1967)
ATS 2 (ALEXANDER et al., 1969)
RAE 1 (FAINBERG & STONE, 1970)
ALOUETTE 1 & 2 (HARTZ, 1969)
AVERAGE CORONA
(SOLAR MIN.)

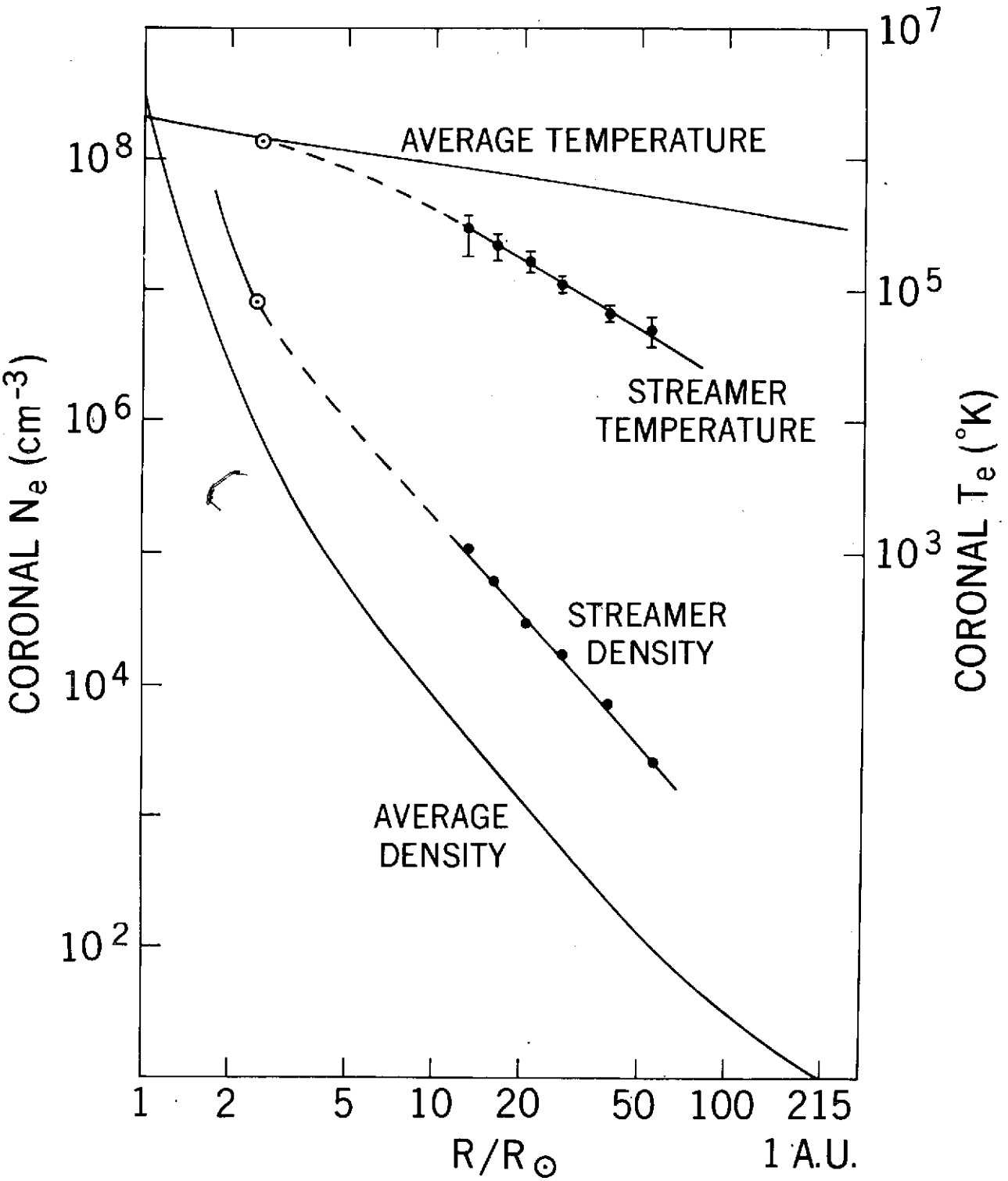
AVERAGE TEMPERATURE
STREAMER TEMPERATURE
STREAMER DENSITY
AVERAGE DENSITY
CORONAL N_e (cm^{-3})
CORONAL T_e (°K)
10^8
10^6
10^4
10^2
10^7
10^5
10^3
1
2
5
10
20
50
100
215
$R/R_\odot$
1 A.U.

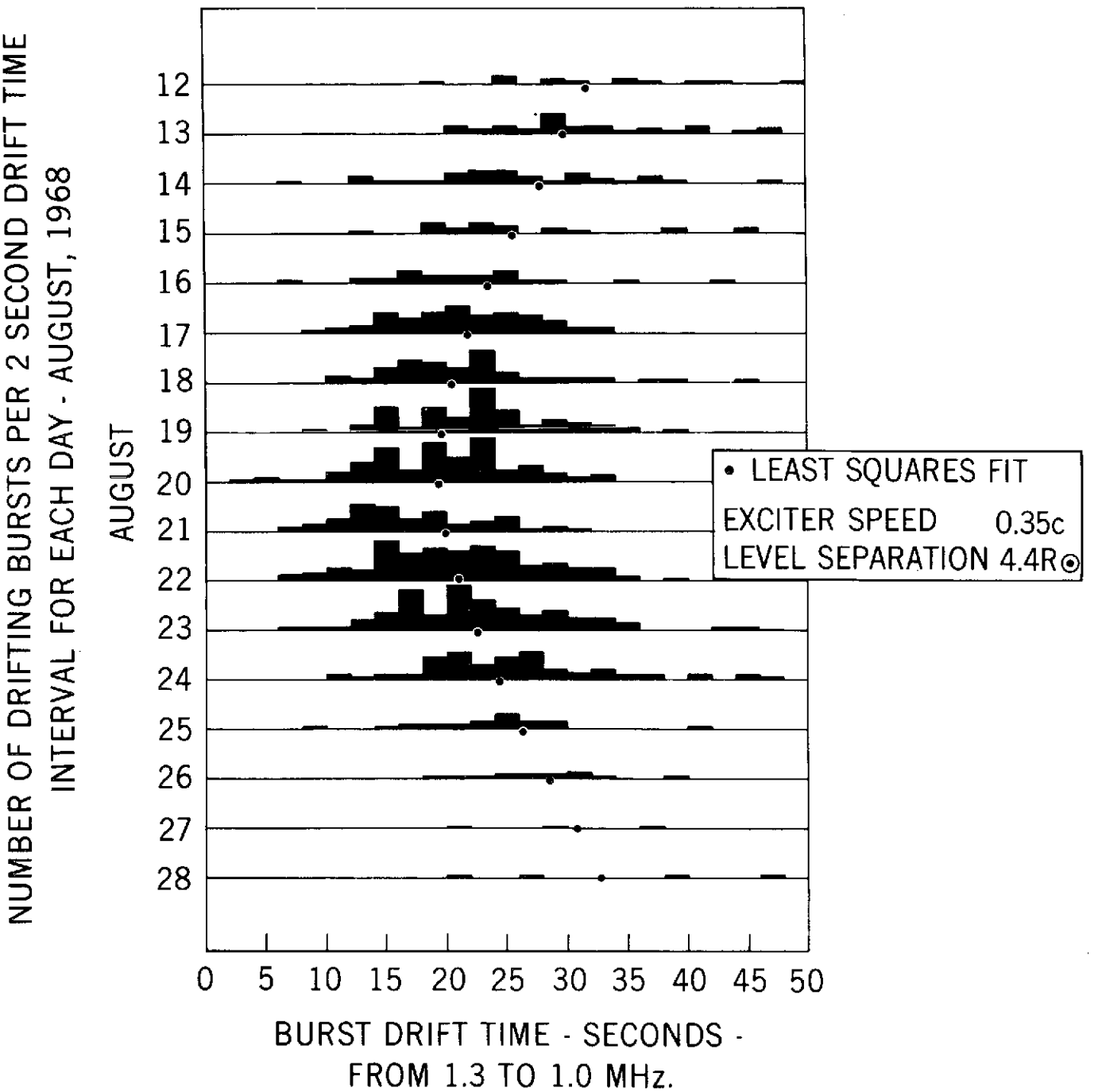
NUMBER OF DRIFTING BURSTS PER 2 SECOND DRIFT TIME INTERVAL FOR EACH DAY - AUGUST, 1968
AUGUST
12
13
14
15
16
17
18
19
20
21
22
23
24
25
26
27
28
• LEAST SQUARES FIT
EXCITER SPEED 0.35c
LEVEL SEPARATION 4.4R⊙
0 5 10 15 20 25 30 35 40 45 50
BURST DRIFT TIME - SECONDS -
FROM 1.3 TO 1.0 MHz.

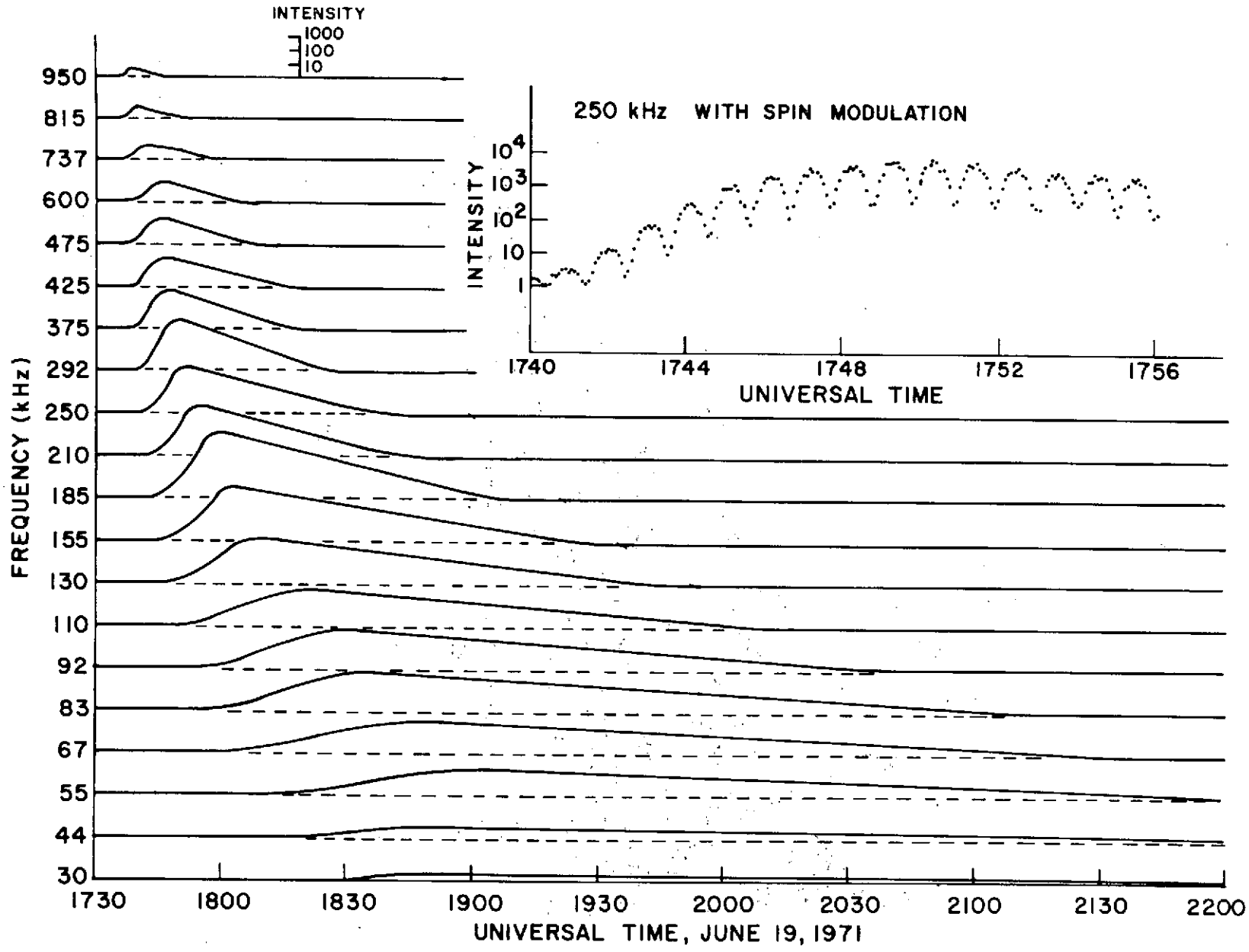
INTENSITY
1000
100
10
950
815
737
600
475
425
375
292
250
210
185
155
130
110
92
83
67
55
44
30
FREQUENCY (kHz)
250 kHz WITH SPIN MODULATION
INTENSITY
10^4
10^3
10^2
10
1
1740
1744
1748
1752
1756
UNIVERSAL TIME
1730
1800
1830
1900
1930
2000
2030
2100
2130
2200
UNIVERSAL TIME, JUNE 19, 1971

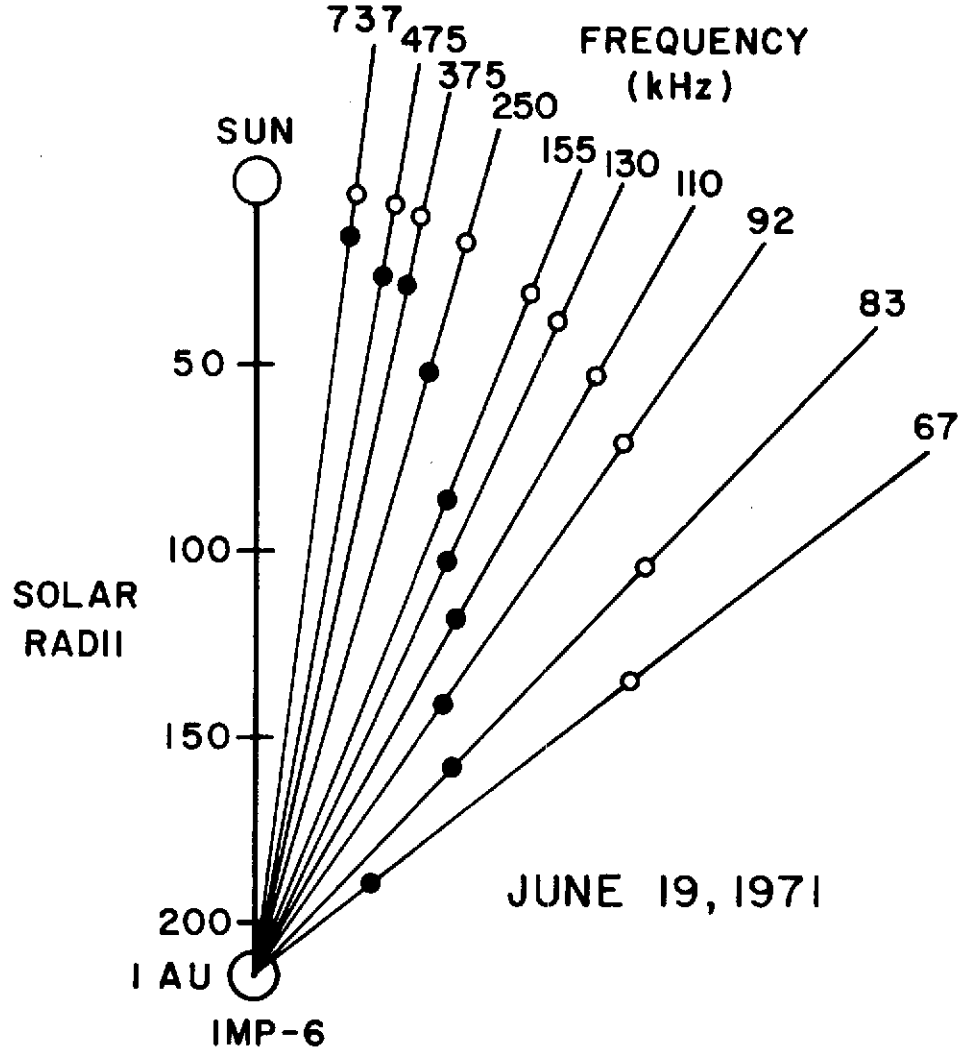
737
475
375
250
155
130
110
92
83
67
FREQUENCY
(kHz)
SUN
50
100
150
200
SOLAR
RADII
1 AU
IMP-6
JUNE 19, 1971

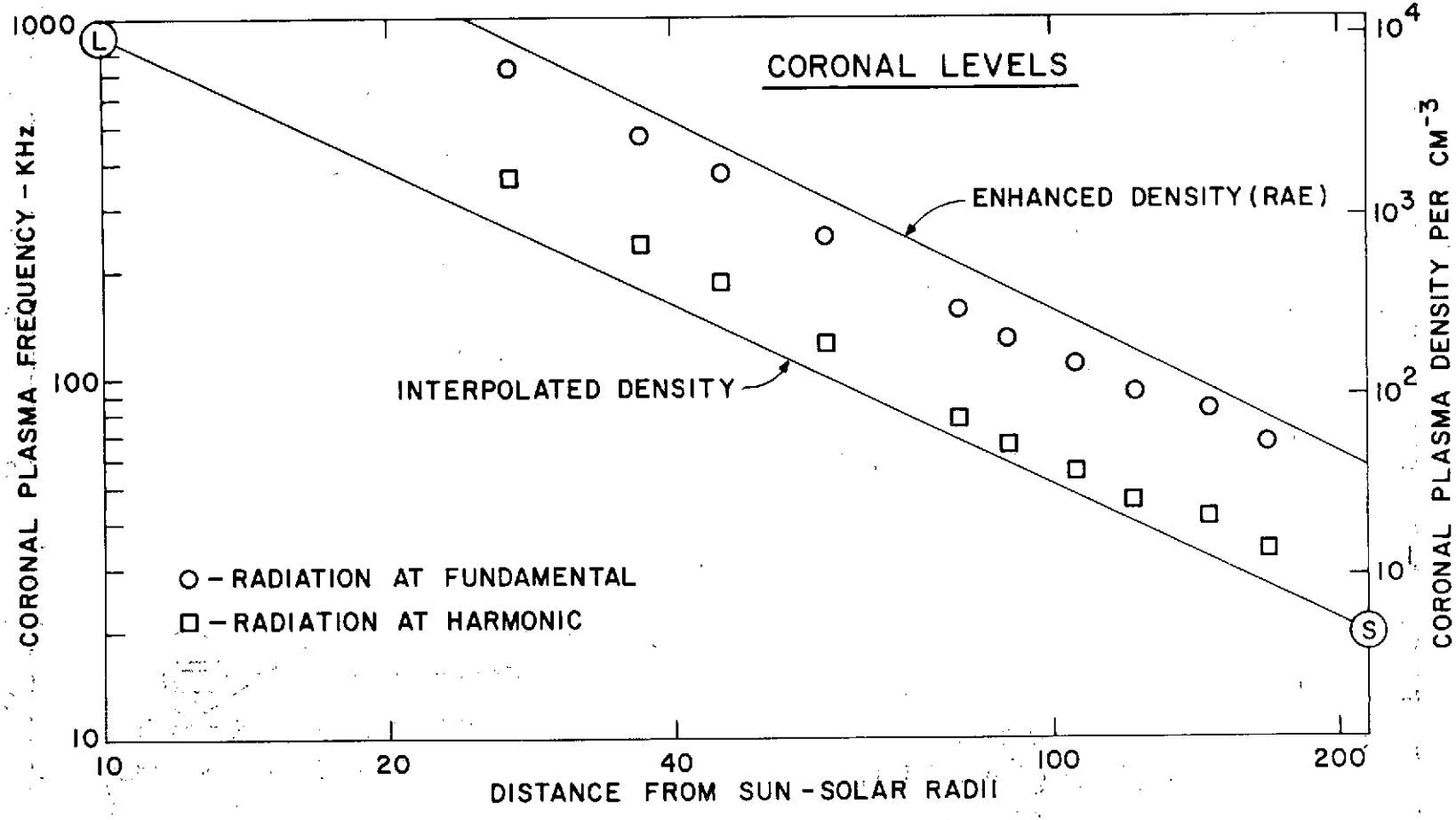
CORONAL LEVELS
ENHANCED DENSITY (RAE)
INTERPOLATED DENSITY
O – RADIATION AT FUNDAMENTAL
□ – RADIATION AT HARMONIC
L
S
1000
100
10
CORONAL PLASMA FREQUENCY – KHz
10^4
10^3
10^2
10^1
CORONAL PLASMA DENSITY PER CM^{-3}
10
20
40
100
200
DISTANCE FROM SUN – SOLAR RADII

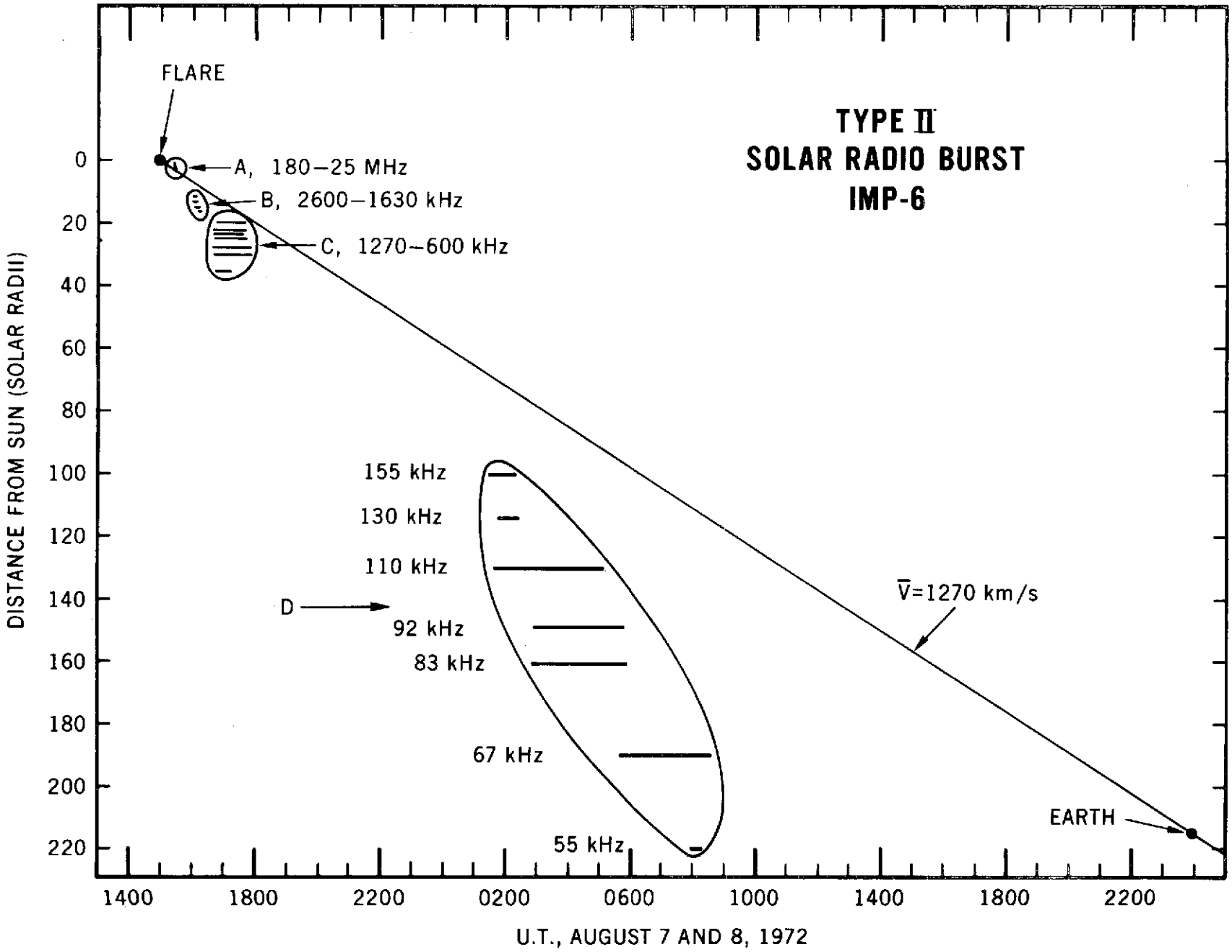
TYPE II
SOLAR RADIO BURST
IMP-6
FLARE
A, 180–25 MHz
B, 2600–1630 kHz
C, 1270–600 kHz
D
155 kHz
130 kHz
110 kHz
92 kHz
83 kHz
67 kHz
55 kHz
V̄=1270 km/s
EARTH
DISTANCE FROM SUN (SOLAR RADII)
0
20
40
60
80
100
120
140
160
180
200
220
1400
1800
2200
0200
0600
1000
1400
1800
2200
U.T., AUGUST 7 AND 8, 1972

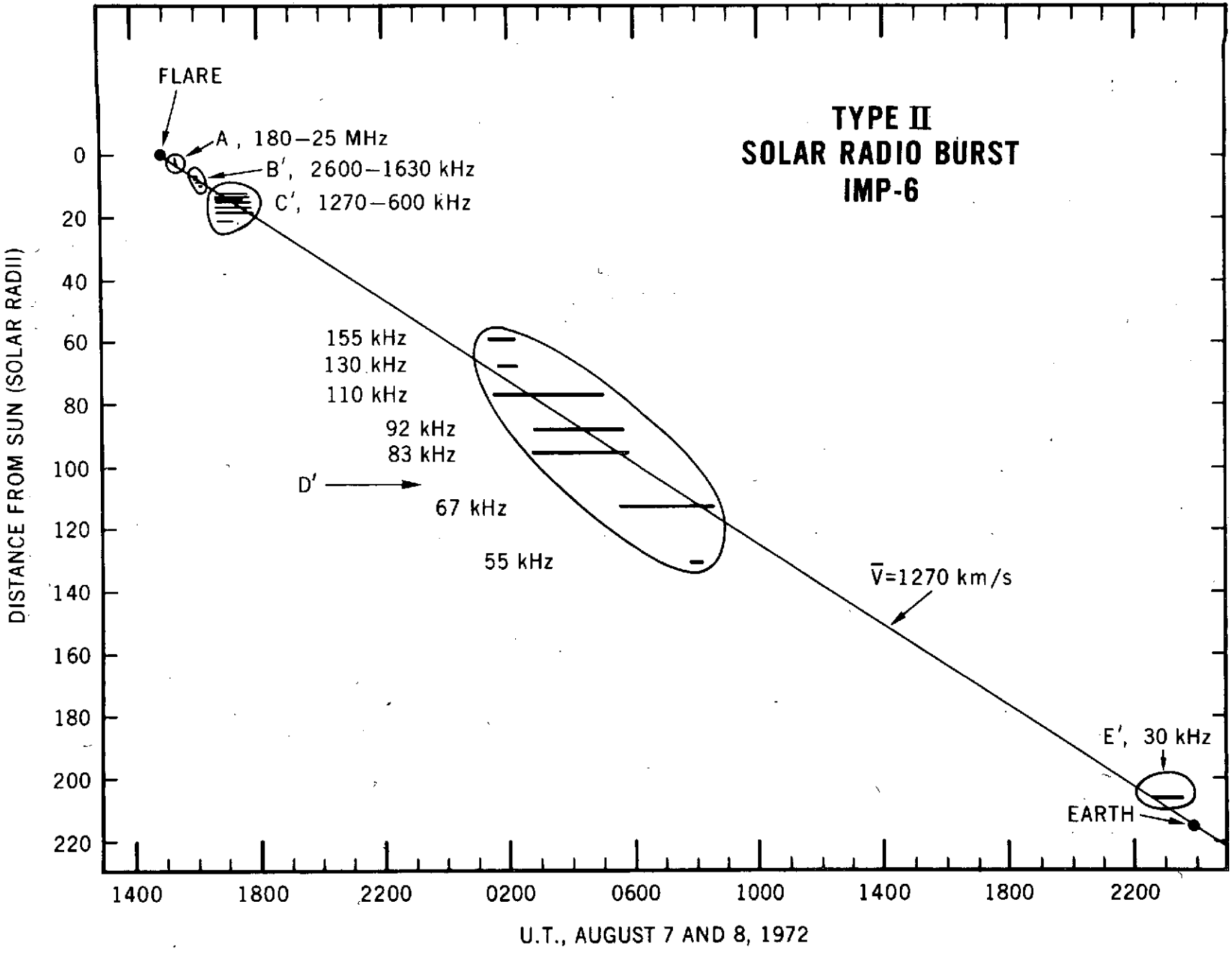
TYPE II
SOLAR RADIO BURST
IMP-6
FLARE
A , 180–25 MHz
B′, 2600–1630 kHz
C′, 1270–600 kHz
155 kHz
130 kHz
110 kHz
92 kHz
83 kHz
D′
67 kHz
55 kHz
V̄=1270 km/s
E′, 30 kHz
EARTH
DISTANCE FROM SUN (SOLAR RADII)
0
20
40
60
80
100
120
140
160
180
200
220
1400
1800
2200
0200
0600
1000
1400
1800
2200
U.T., AUGUST 7 AND 8, 1972

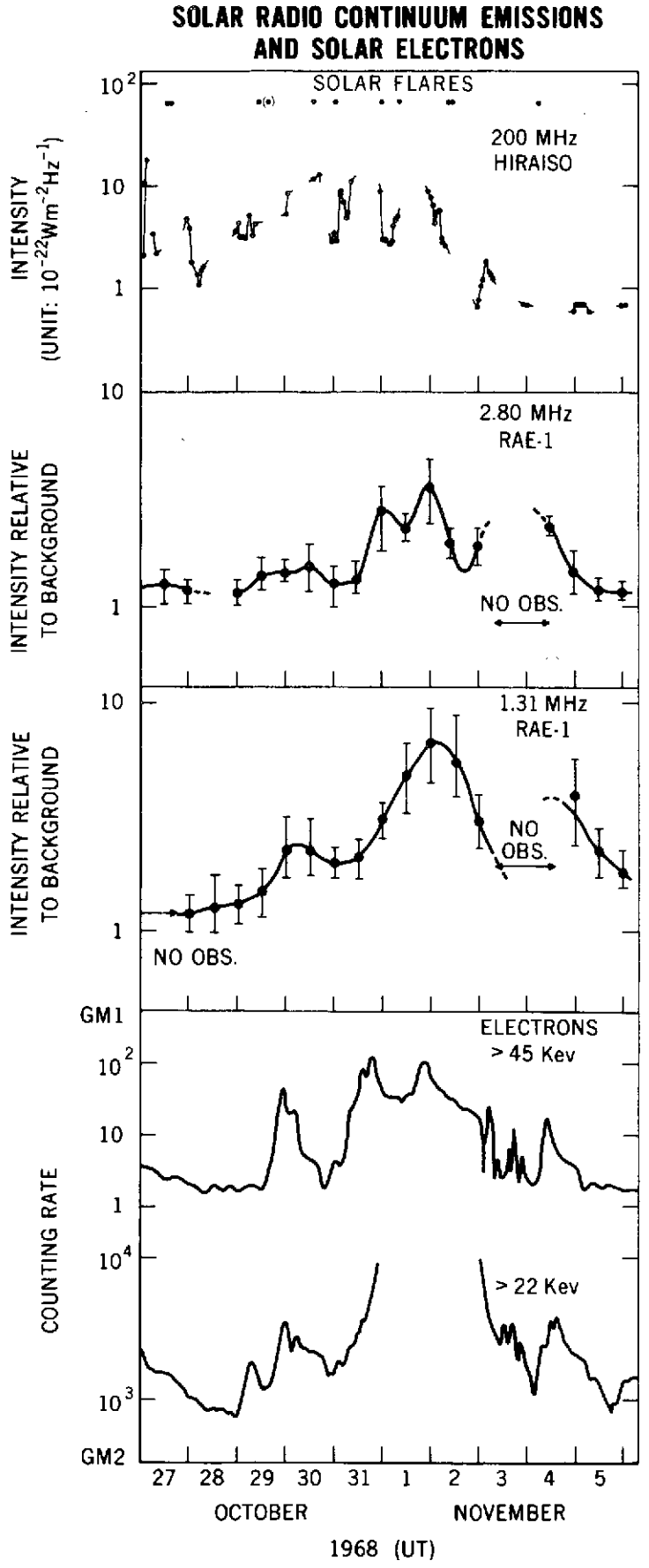
SOLAR RADIO CONTINUUM EMISSIONS
AND SOLAR ELECTRONS
SOLAR FLARES
200 MHz
HIRAISO
INTENSITY
(UNIT: 10^{-22}Wm^{-2}Hz^{-1})
10^2
10
1
10
2.80 MHz
RAE-1
INTENSITY RELATIVE
TO BACKGROUND
NO OBS.
1.31 MHz
RAE-1
NO
OBS.
NO OBS.
GM1
ELECTRONS
> 45 Kev
COUNTING RATE
10^4
> 22 Kev
10^3
GM2
27 28 29 30 31 1 2 3 4 5
OCTOBER
NOVEMBER
1968 (UT)

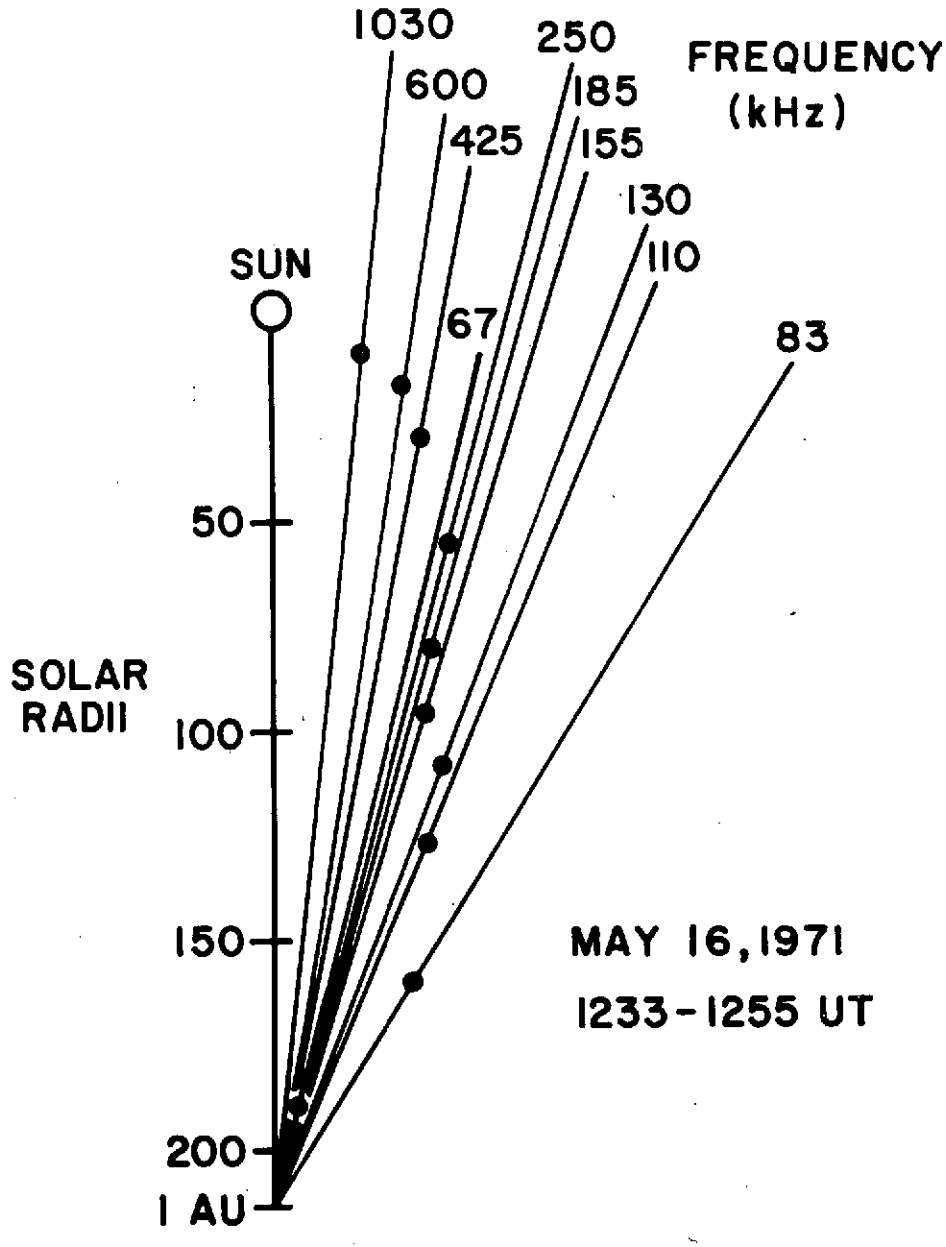
1030
600
425
250
185
155
130
110
83
67
FREQUENCY
(kHz)
SUN
50
100
150
200
1 AU
SOLAR
RADII
MAY 16, 1971
1233-1255 UT

C2

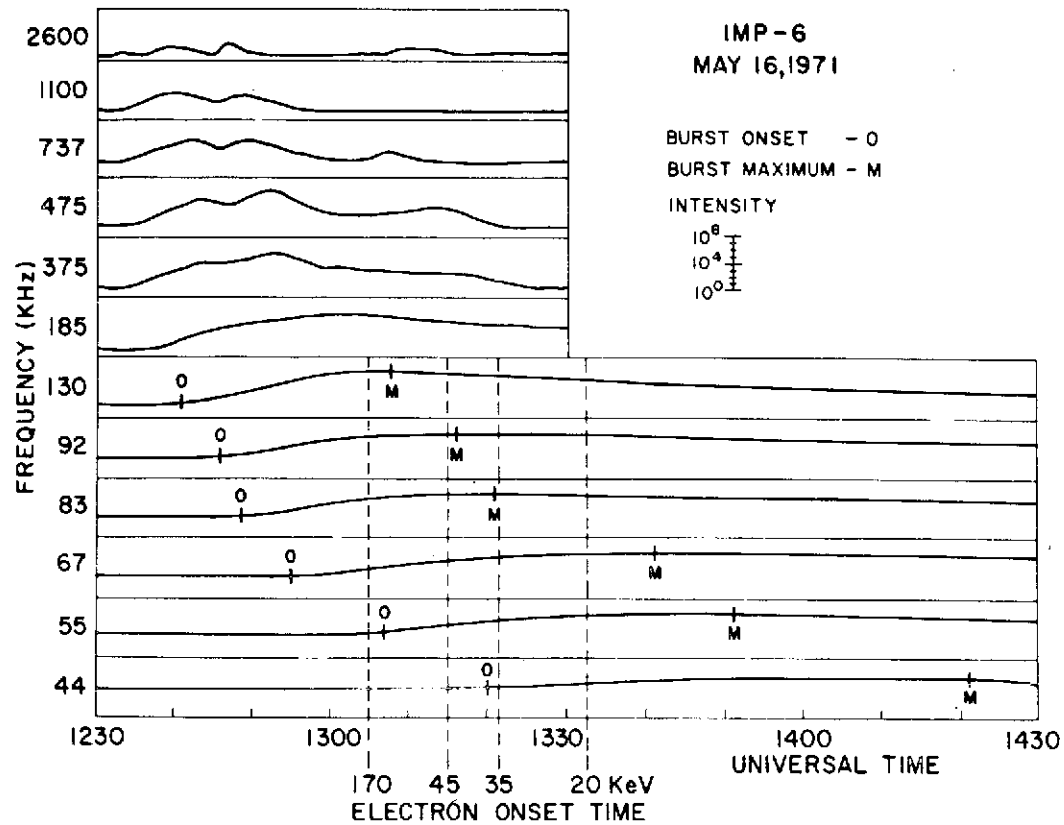
IMP-6
MAY 16,1971
BURST ONSET - O
BURST MAXIMUM - M
INTENSITY
10^6
10^4
10^0
FREQUENCY (KHz)
2600
1100
737
475
375
185
130
92
83
67
55
44
O
M
1230
1300
1330
1400
1430
UNIVERSAL TIME
170 45 35 20 KeV
ELECTRON ONSET TIME

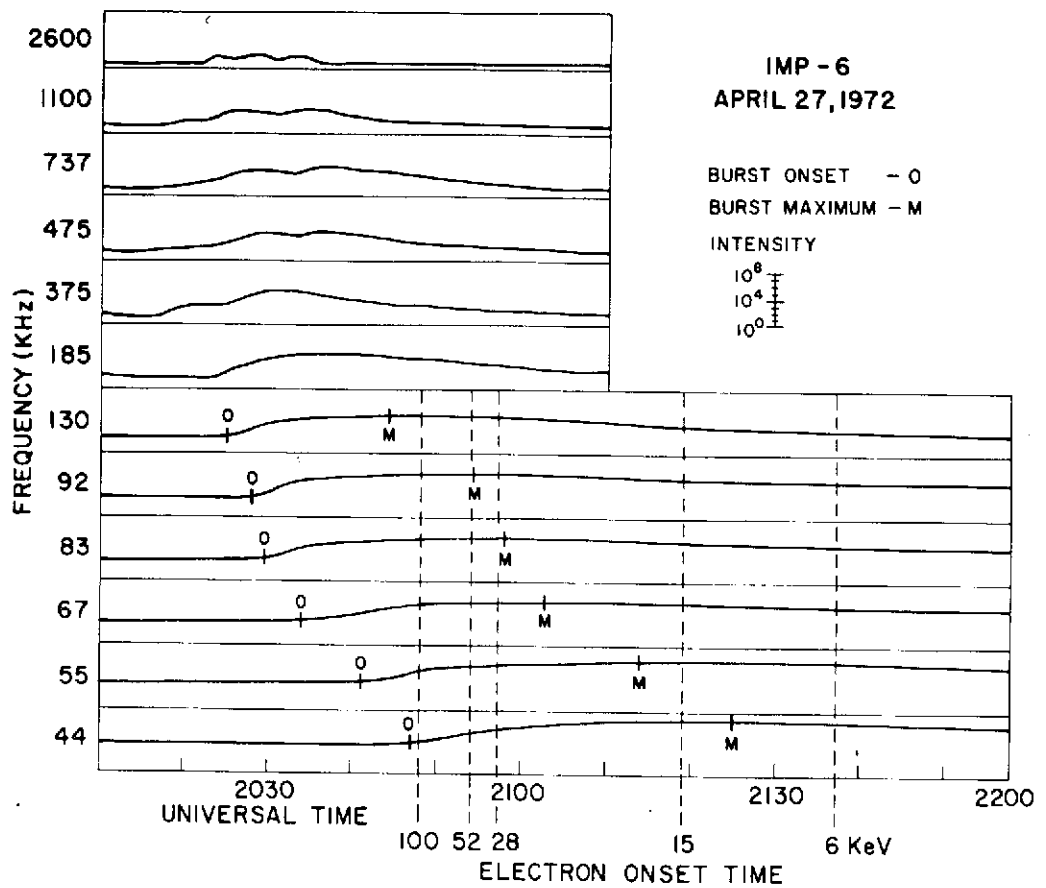
IMP-6
APRIL 27,1972
BURST ONSET - O
BURST MAXIMUM - M
INTENSITY
10^6
10^4
10^0
FREQUENCY (KHz)
2600
1100
737
475
375
185
130
92
83
67
55
44
O
M
2030
UNIVERSAL TIME
2100
2130
2200
100 52 28
15
6 KeV
ELECTRON ONSET TIME

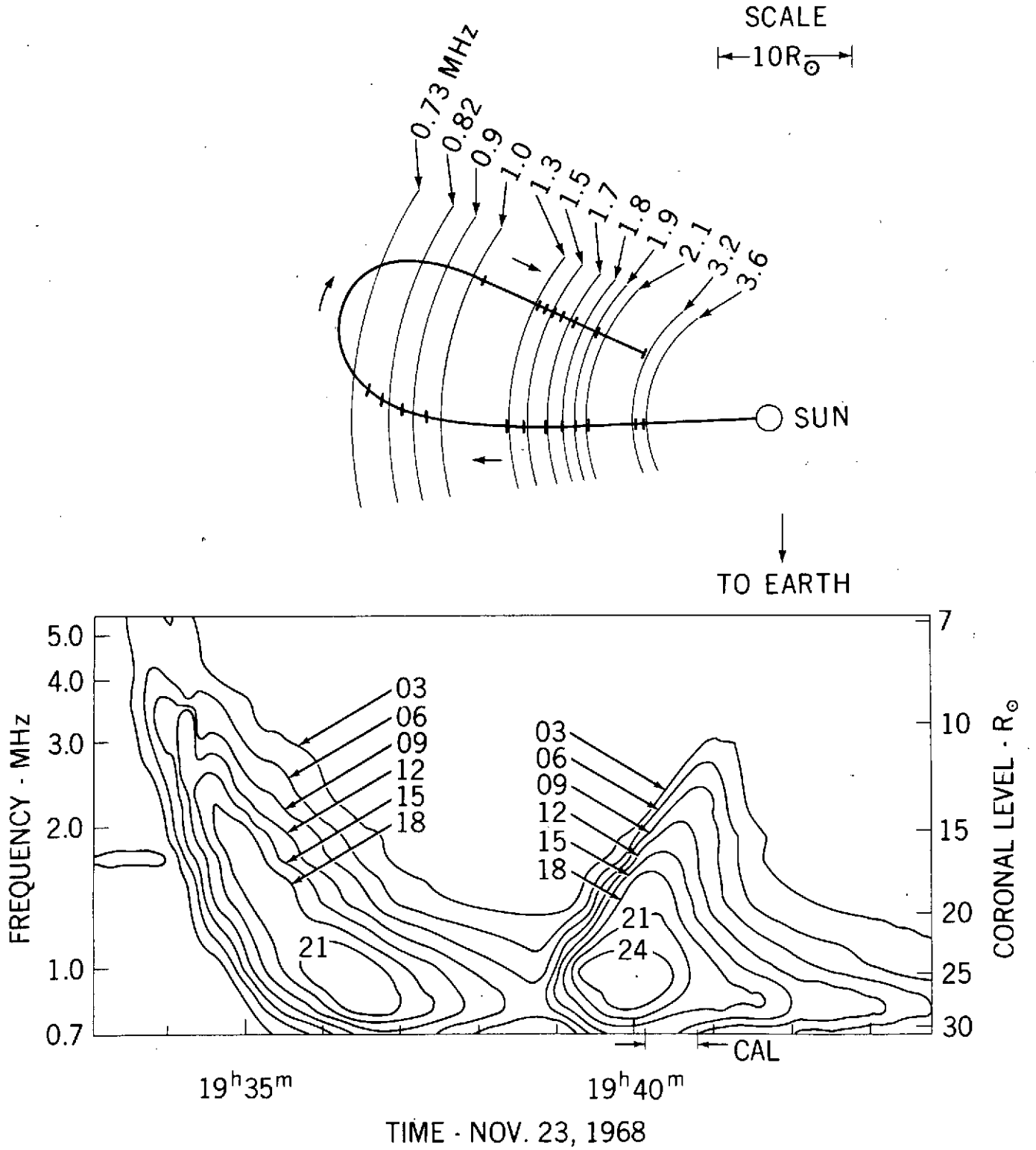
SCALE
10R⊙
0.73 MHz
0.82
0.9
1.0
1.3
1.5
1.7
1.8
1.9
2.1
3.2
3.6
SUN
TO EARTH
5.0
4.0
3.0
2.0
1.0
0.7
FREQUENCY - MHz
03
06
09
12
15
18
21
03
06
09
12
15
18
21
24
CAL
7
10
15
20
25
30
CORONAL LEVEL - R⊙
19h35m
19h40m
TIME - NOV. 23, 1968

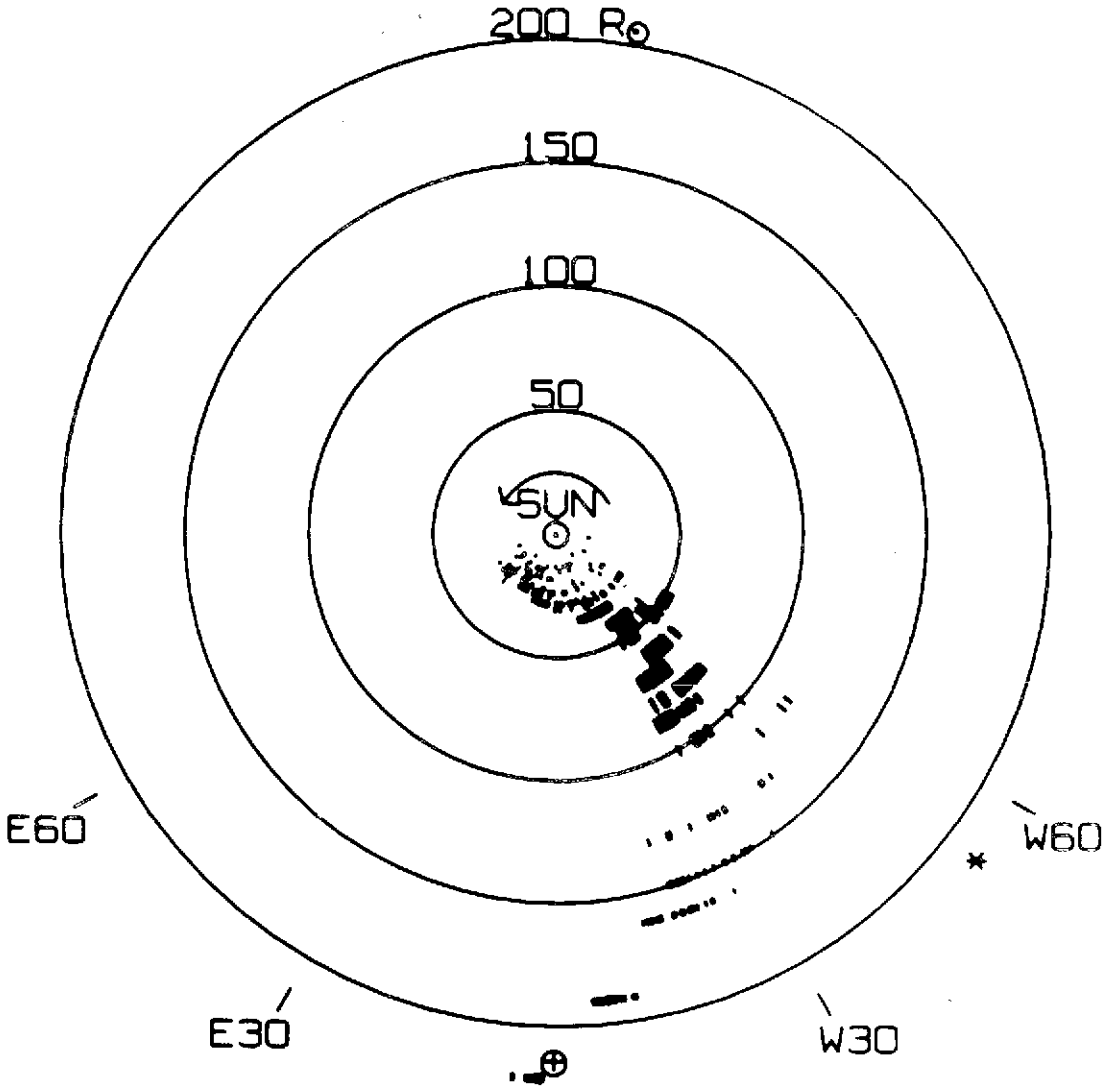

IMP-6 ϵ EARTH

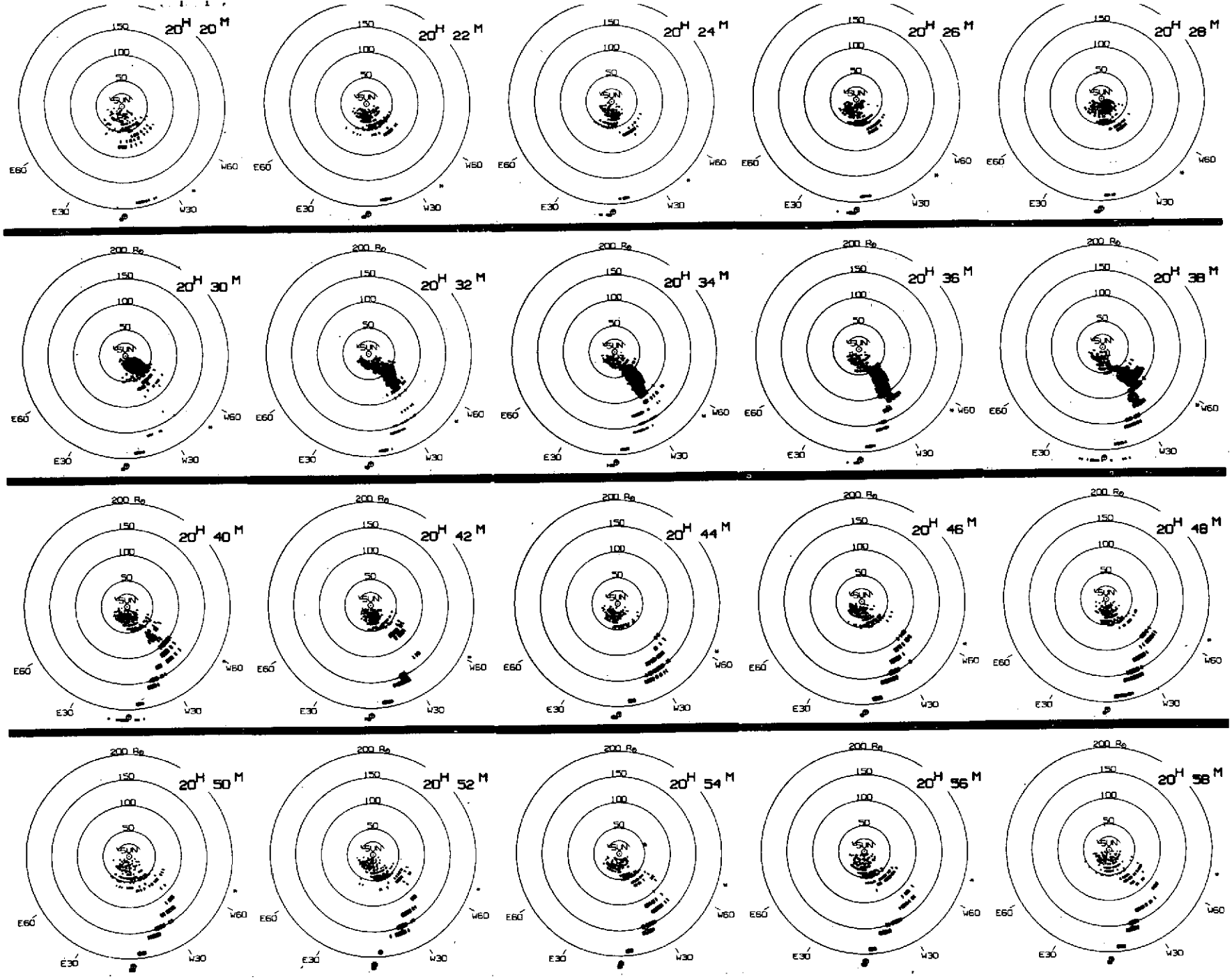
20H 20M
20H 22M
20H 24M
20H 26M
20H 28M
20H 30M
20H 32M
20H 34M
20H 36M
20H 38M
20H 40M
20H 42M
20H 44M
20H 46M
20H 48M
20H 50M
20H 52M
20H 54M
20H 56M
20H 58M
200 Re
150
100
50
SUN
E60
E30
W30
W60

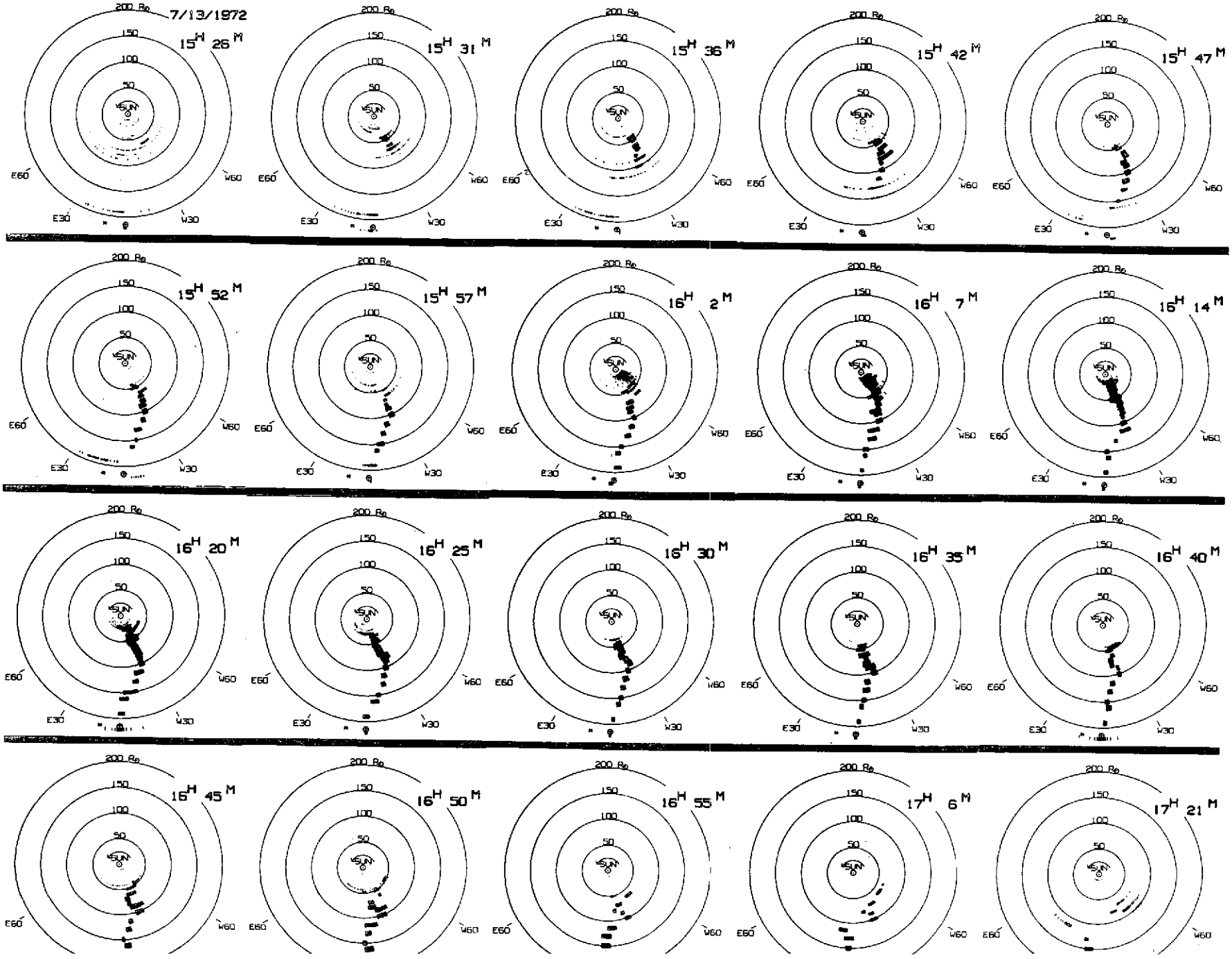
7/13/1972
15H 26M
15H 31M
15H 36M
15H 42M
15H 47M
15H 52M
15H 57M
16H 2M
16H 7M
16H 14M
16H 20M
16H 25M
16H 30M
16H 35M
16H 40M
16H 45M
16H 50M
16H 55M
17H 6M
17H 21M
200 RE
150
100
50
SUN
E60
E30
W30
W60

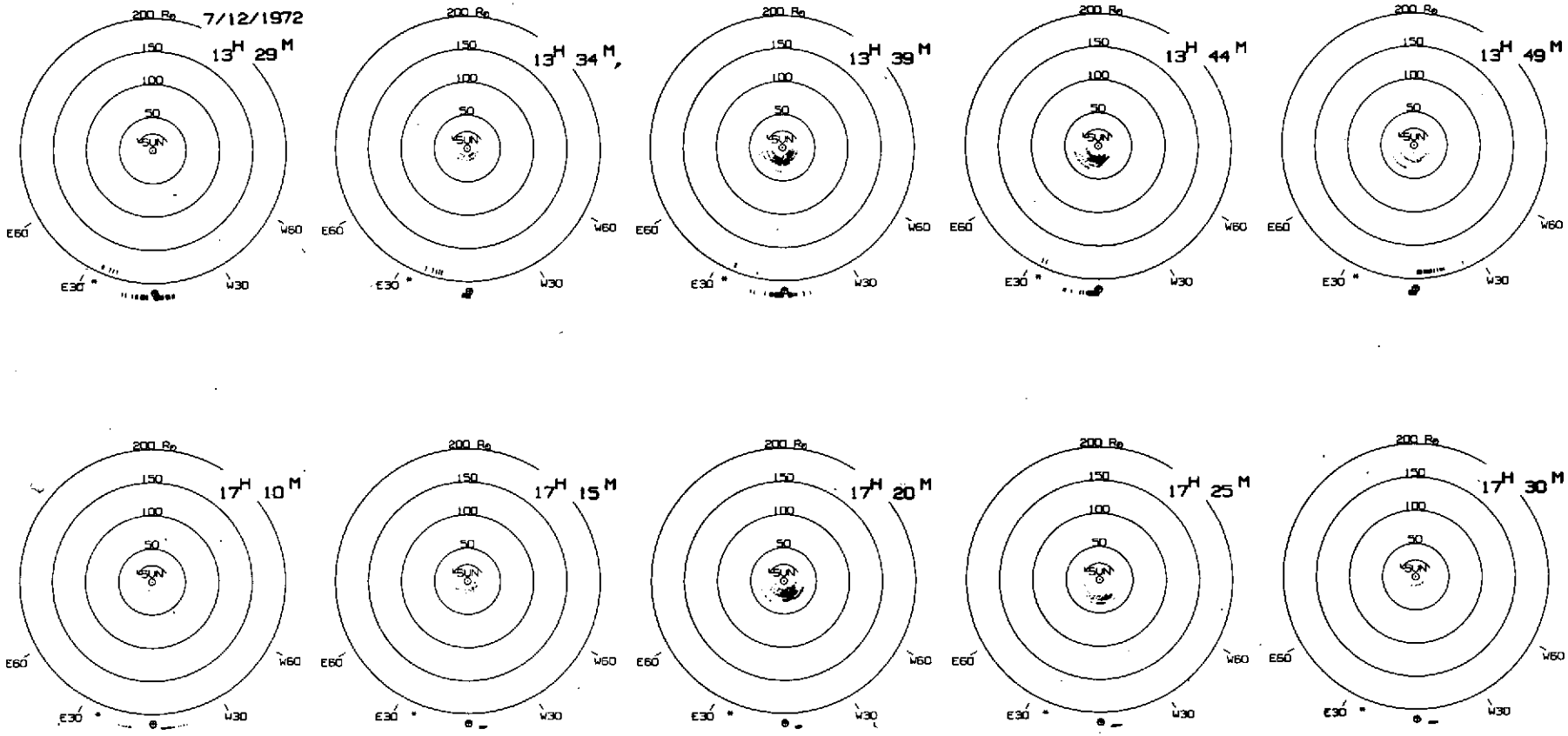
7/12/1972
13H 29M
13H 34M
13H 39M
13H 44M
13H 49M
17H 10M
17H 15M
17H 20M
17H 25M
17H 30M
200 Rs
150
100
50
SUN
E60
W60
E30
W30

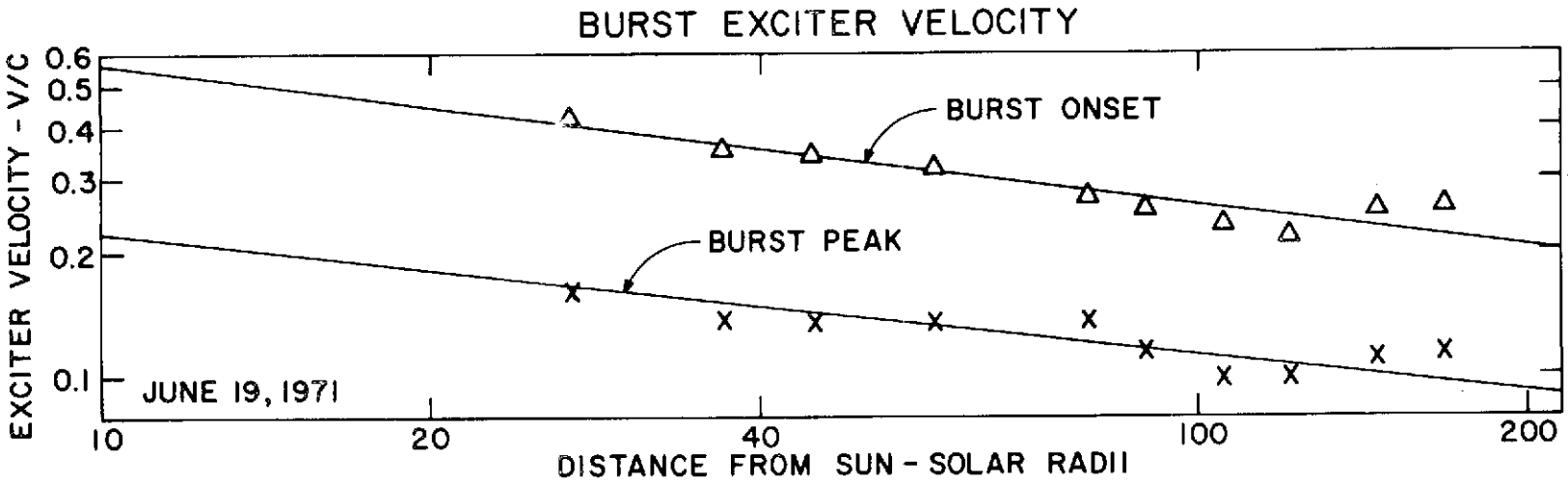
BURST EXCITER VELOCITY
EXCITER VELOCITY - V/C
0.6
0.5
0.4
0.3
0.2
0.1
BURST ONSET
BURST PEAK
JUNE 19, 1971
10
20
40
100
200
DISTANCE FROM SUN - SOLAR RADII

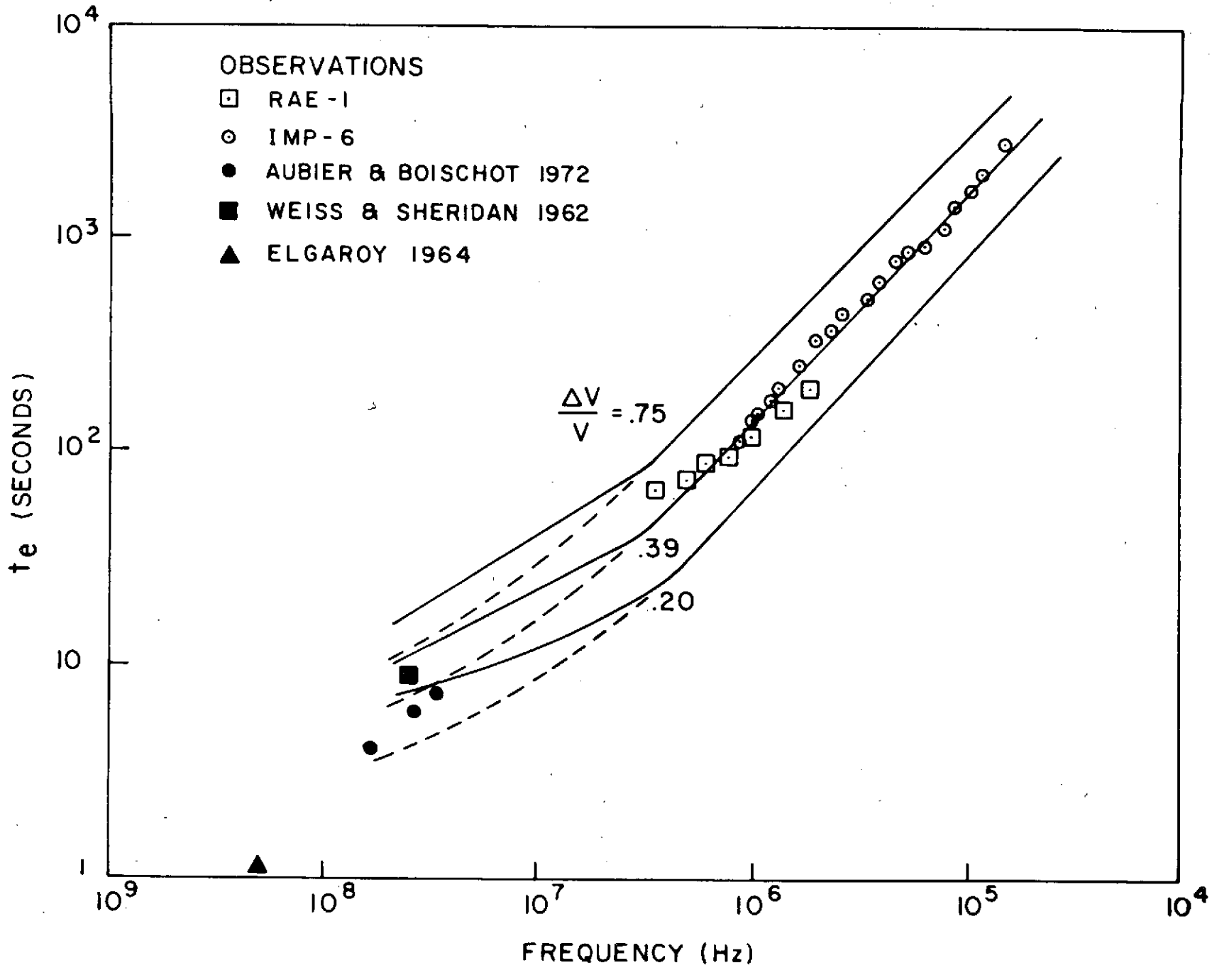
OBSERVATIONS
RAE-1
IMP-6
AUBIER & BOISCHOT 1972
WEISS & SHERIDAN 1962
ELGAROY 1964
ΔV/V = .75
.39
.20
te (SECONDS)
FREQUENCY (Hz)
10^4
10^3
10^2
10
1
10^9
10^8
10^7
10^6
10^5
10^4